

# ON STOCHASTIC DYNAMIC PREDICTION

## I. The Energetics of Uncertainty and the Question of Closure

REX J. FLEMING

Air Weather Service, U.S. Air Force<sup>1</sup>

### ABSTRACT

In this, the first part of a two-part study, we examine the rationale of the stochastic dynamic approach to numerical weather prediction. Advantages of the stochastic dynamic method are discussed along with problems associated with the method. This method deals with the initial uncertainty by considering an infinite ensemble of initial states in phase space, relative frequencies within the ensemble being proportional to probability densities. The evolution of this ensemble in time, given by the stochastic dynamic equation set, is based upon the original deterministic hydrodynamic equation set. One may consider the latter set as a subset of the former. Insight into the nature of these equations is obtained by deriving the energy transformations associated with them. A simple baroclinic model is used to isolate the energy concepts and relations. The energetics yield qualitative and quantitative information on the nature of the growth of uncertainty. It is found that the baroclinic instability mechanism is responsible for most of the error growth as would be expected.

Previous predictability studies have considered that the simulation of the forces governing the atmosphere has been perfect. The effects of imperfect forcing can be viewed with the stochastic dynamic equations by adding another dimension to phase space for each parameter considered to be uncertain. The effect of the inclusion of this imperfect forcing is shown by the new energetic relations that result, and by numerical calculation of the changes in the growth of uncertainty.

The stochastic dynamic equations are faced with the same mathematical problem of "closure" found in analytical treatments of homogeneous isotropic turbulence; that is, an approximation concerning higher order moments must be made to close the system. A number of closure schemes are studied and it is found that the third moments, which are individually small, should nevertheless be retained. It is shown in the equations and verified by numerical calculations that the third moments do not affect energy conservation but affect energy conversion between uncertain components, with the eventual result of altering the forecast of the mean. An eddy-damped third moment scheme is found to give extremely accurate results when compared to Monte Carlo calculations.

### 1. INTRODUCTION

There is considerable interest today in the limits of predictability of the atmosphere. Perhaps a more relevant concern than the "limit" is what the practical predictability values will be for the various scales of atmospheric features in the near future, say, 1, 5, or 10 yr from now.

What effort must be expended to achieve what degree of predictability? This study is concerned with a method that can deal with the above concern. Moreover, a more profound question that some meteorologists must eventually ask themselves is, "What course does numerical prediction follow after these practical limits of predictability for the various features have been reached?"

One answer to the above question is to use the uncertainty of the forecast itself as information. Certainly, the variance or uncertainty of any meteorological variable is important information, and may be as valuable as the forecast of the variable itself. A technique for coping with the uncertainties that exist in the initial conditions of a numerical forecast is explicitly given in the method of stochastic dynamic prediction (Epstein 1969b).

In numerical weather prediction, there are several sources of uncertainty that are part of the mathematical

initial-value problem. Acknowledging these sources, the stochastic dynamic formulation of that problem forecasts the expected value and uncertainty of every meteorological variable at each point in the space domain and at every instant of time. No assumptions are made concerning the physics of the original problem.

Some of the uncertainties that exist in the numerical forecasts are due to errors in the initial conditions. A list (by no means exhaustive) of sources of uncertainty in the initial conditions of a numerical forecast might be: errors in the raw data (instrument, transmission, etc.), errors arising from the heterogeneous data set whose signal only partially describes the complete inertial-gravity wave and turbulence phenomena that exist at a particular instant in the atmosphere, errors caused by the complete absence of scales of motion unresolved by the paucity of the data, "random" analysis error (Thompson 1957) arising from the reconstruction of the grid analysis from a finite number of data points, errors caused by loss of significant kinetic energy near the jet stream from smoothing by the analysis technique, and that due to further smoothing of the smaller scales that is usually necessary to avoid amplification (beyond physical reality) of the short-wave-length components.

The above are some of the errors that will limit the practical value of predictability. In addition, the numerical

<sup>1</sup> Now assigned to the National Meteorological Center, National Weather Service, NOAA, Suitland, Md.

models used in forecasting are not perfectly simulating the physical processes of the atmosphere. Indeed, some of these processes have not yet been fully explained. This obviously decreases the practical value of predictability.

If one could assume that all the above errors could be eliminated and, in addition, if it could be assumed that the physics of the atmosphere were "perfectly" known and/or could be perfectly parameterized for numerical computation, one would still be faced with a source of error. The hydrodynamic fields must be represented in a finite manner—in terms of a space mesh or in terms of orthogonal coefficients. Thus, the smallest scales of motion that are unresolved must be ignored or treated statistically. However, the nonlinearity of the equations causes statistically treated small scales to give a random perturbation to the motions of the large scales, causing these scales to be increasingly unpredictable with time. This "aliasing effect," which is summarized by Leith (1969), increases computational instability. The computational instability can be dealt with in a number of ways (using a filtering technique at various points in time, using a finite-difference scheme that inherently smooths, using an artificial viscosity); however, the generation of uncertainty at higher scales still remains. It is this last type of uncertainty that is generally felt to be responsible for the limit of predictability of various scales.

The nonlinear interactions between scales (known and unknown), coupled with physical forces that are not perfectly understood, produce uncertainty and make statements of practical predictability only "speculation" when the usual meteorological equations are used.

The stochastic approach to predicting the atmosphere appears to be capable of reducing that speculation of predictability. Consider a model of the atmosphere described by a certain number of variables. A stochastic model would specify the complete joint probability distribution of all the variables at each point in time, and the whole process conceived as a continuous development in time would be a stochastic method.

The model equations used in predicting the atmosphere are assumed to be deterministic; that is, the exact present state of the dependent variables completely determines the exact future state of those variables. Since the initial conditions of the atmosphere are known only in a probabilistic sense, Epstein's method seems appropriate. As will be seen later in the paper, the deterministic equations are but a subset of the stochastic equations and, thus, a tremendous amount of computer power is required to utilize the stochastic set. There remain some fundamental problems and questions to be solved and answered before these equations can be incorporated on a practical basis.

The purpose of this paper is to resolve those problems and questions left open in the paper of Epstein (1969b). The rationale of the stochastic dynamic equations will be critically evaluated. The physical meaning of the relationships that exist within these equations will be discussed for the first time. An energy diagram will be derived which shows the energetic relationships that

must exist in any prediction or simulation model in which an account of the uncertainties is made.

The stochastic dynamic equations are actually an infinite unclosed set of coupled equations which cannot be solved until a method of closing them is devised. This question of "closure" is dealt with and is viewed in analytical terms.

Freiberger and Grenander (1965) discuss the same problem that this paper is concerned with—how to *deal with* the uncertainties that limit predictability, rather than what the limit of predictability is. They propose stochastic solutions to "limited" problems using an approach analogous to classical statistical mechanics. They did not offer the *means* to the solution of the complex atmospheric equations, but stated what form that solution should take. A relevant quote from their paper is: "Starting from the dynamic equations, whether in their primitive or in a modified form, we should consider an ensemble of possible solutions. The uncertainties and lack of completeness of our initial weather data would then correspond to a probabilistic superstructure on the ensemble. . . . The conceptual, analytical and numerical difficulties inherent in this approach are so overwhelming that prospects of a completely successful analysis seem remote."

It is hoped that the present study is a significant step toward unraveling those conceptual, analytical, and numerical difficulties.

## 2. THE STOCHASTIC DYNAMIC EQUATIONS

To visualize the difference between a deterministic and stochastic dynamic forecast of a system, consider that there are  $N$  dependent variables describing the system. The deterministic prognostic equations can be expressed in the general form

$$dX_i/dt = F_i(X_1, X_2, X_3, \dots, X_N) \quad (1)$$

where the  $X_i$  are the  $N$  dependent variables describing the system. The  $N$  variables form an  $N$ -dimensional Euclidean space whose coordinates are  $X_1, \dots, X_N$ . Such a space is called a phase space, where each point in the phase space represents a possible instantaneous state of the system.

The initial state of the atmosphere is then represented by a single point in the phase space and the deterministic forecast gives the trajectory of that point in phase space. In figure 1, the  $N$ -dimensional phase space is represented by any two dimensions. In this figure, point S is the initial position of a single point in phase space and S' is a point on the deterministic trajectory of that same point at a later time  $t_i$ .

The results of all the possible uncertainties in the final numerical analysis leads to a great number of possible initial states in the previously defined  $N$ -dimensional phase space. Each of the different initial states will yield a different trajectory in phase space even though subjected to the same set of prognostic equations. Slightly

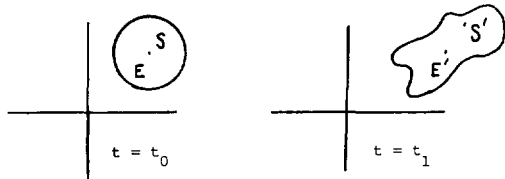


FIGURE 1.—Evolution of a point and an ensemble in phase space.

different initial states may yield significantly different trajectories. This is to be expected in light of Lorenz' (1963a) discussion of nonperiodic trajectories. He concludes that two atmospheric states differing by imperceptible amounts may eventually evolve into two considerably different states.

Is there a way to know which initial state is the correct one? Were the matter of initializing the dependent variables of the atmosphere merely a question of inaccurate random measurements, then, in theory, an average of an *infinite* set of measurements would converge to the "true" state. However, operational predictions depend upon a single set of data and it is impossible to know the actual error. Moreover, the determination of the proper initial conditions of the *numerical prediction* problem is more complex than the theory of random measurements.

Consider an observing net with the same data density as exists today or even as it might exist 10 yr from now. Even if each individual observation were a perfect representation (Heisenberg's Principle of Uncertainty ignored for the moment), such data would not be acceptable as initial conditions of the numerical prediction model. Each measured signal would be a superposition of many atmospheric modes, some for which a *complete* spatial description could not be given by the coarse data resolution. Indeed, this is why the microscale features, inertial-gravity wave oscillations, turbulence, etc., are smoothed and/or modified in the final numerical analysis. The analysis is made physically and computationally consistent with the numerical model. From the viewpoint of the model, then, there is no true initial state of the *atmosphere*. However, there ought to exist some state which is at least statistically optimal and consistent with the objectives of the numerical prediction scheme.

The fact that the observations do have errors further complicates the selection of that optimal initial state which is consistent with the intentions of the prediction model. It seems logical, then, to express the initial conditions in terms of a probability distribution. This would mean considering an infinite ensemble of initial states in phase space with relative frequencies within the ensemble proportional to the probability densities. This initial joint probability distribution will evolve in a nonlinear manner according to the dynamic equations. It will be seen that the stochastic method only forecasts the low-order moments of that distribution, and that the lowest order moments, the means, are by definition the

"expected values" of the dependent variables consistent with the original analysis, all the uncertainties, and the nonlinear dynamic processes at work during the length of the forecast.

Such an ensemble is shown in figure 1 where E and S coincide and the ensemble mean, E, evolves to E'. Because of the nonlinearities, there will eventually be a time  $t_1$  where E' and S' would differ. This is seen in independent Monte Carlo and stochastic dynamic calculations presented in the latter portion of this paper and is also discussed by Epstein (1969a, 1969b).

How one might obtain an approximation of the *initial* joint probability distribution or, at least, of the low-order moments of that distribution will not be the subject of this paper. For our purposes, we shall consider that by some method (deterministic or stochastic) the best possible physically consistent analysis has been made. Because of all the associated uncertainties, we consider the analyzed values of the  $N$  variables to be expected values having a variance or measure of uncertainty associated with each.

There remains the problem of determining the evolution of the ensemble. In terms of the atmospheric prediction problem, this has recently been accomplished independently and at about the same time by Tatarskii (1969) and Epstein (1969b). The final result of each author was the same, but each had a different conceptual basis for the technique and each had a different interpretation of the result. Both authors advocate using the dynamic equations to find the probability distribution of future meteorological fields, not the complete probability density distribution over the entire phase space—this is an impossible task—but only the first and second moments of the distribution over phase space. Both drop third and higher order moments to close the system of equations.

Tatarskii uses a simple nonlinear form of a prediction equation and from it derives the Liouville equation describing the evolution of the probability density. Epstein considers the one-dimensional probability equation of Gleeson (1966) but extends it to  $N$ -dimensions, corresponding to the  $N$ -dimensional phase space under consideration. This equation is exactly the same as Tatarskii's Liouville equation. Epstein calls his equations the "stochastic dynamic" set of equations for the atmosphere. This nomenclature is adopted here. Epstein presents numerical results using a simple barotropic model with only eight orthogonal functions representing the space domain, where the amplitudes of these orthogonal functions are functions of time. He drops third and higher order moments and calls the resulting equations the "approximate" stochastic dynamic equations.

Consider writing the hydrodynamic equations in the general form given by Lorenz (1963a) as

$$\dot{X}_i = \sum_{p,q} a_{ipq} X_p X_q - \sum_p b_{ip} X_p + c_i \quad (2)$$

where  $p$  and  $q$  are dummy indices,  $(\dot{\phantom{x}})$  refers to a time derivative, and the  $a$ 's,  $b$ 's, and  $c$ 's are constants describing

nonlinear interactions, external forces, and dissipative mechanisms. The dependent variables,  $X_i$ , could be grid point values or amplitudes of orthogonal functions, in principle, but the latter form of specifying the spatial dependence will be used here. From the definition of expectation, the expected value of  $f(X)$  at time  $t$  is given by

$$E[f(\tilde{X})] = \int_{-\infty}^{\infty} f(\tilde{X}) \phi(\tilde{X}, t) d\tilde{X} \quad (3)$$

where  $d\tilde{X} = dX_1, dX_2, \dots, dX_N$  and  $\phi(\tilde{X}, t)$  is the probability density that satisfies

$$\int \dots \int \phi(\tilde{X}, t) dX_1, dX_2, \dots, dX_N = 1$$

over the phase space. One can then derive the following relationships for  $X_i$ , any variable of the set of variables  $X_N$  that makes up the phase space:

$$E(X_i) = \mu_i, \quad (4)$$

$$E(X_i X_j) = \mu_i \mu_j + \sigma_{ij}, \quad (5)$$

$$\text{and} \quad E(X_i X_j X_k) = \mu_i \mu_j \mu_k + \mu_i \sigma_{jk} + \mu_j \sigma_{ik} + \mu_k \sigma_{ij} + \tau_{ijk} \quad (6)$$

where:

$\mu_i$  is the mean of  $X_i$ ,

$\sigma_{ij}$  is the variance if  $i=j$ , covariance if  $i \neq j$ ,

$\tau_{ijk}$  is the instantaneous third moment about the mean,

and where  $X_i, \mu_i, \sigma_{ij}, \tau_{ijk}$  are all functions of time. The equations for the means and the second moments about the means corresponding to the deterministic set [eq (2)] have been derived by Epstein (1969b):

$$\dot{\mu}_i = \sum_{p,q} a_{ipq} (\mu_p \mu_q + \sigma_{pq}) - \sum_p b_{ip} \mu_p + c_i \quad (7)$$

$$\text{and} \quad \dot{\sigma}_{ij} = \sum_{p,q} [a_{ipq} (\mu_p \sigma_{jq} + \mu_q \sigma_{jp} + \tau_{jpq}) + a_{jqp} (\mu_p \sigma_{iq} + \mu_q \sigma_{ip} + \tau_{ipq})] - \sum_p (b_{ip} \sigma_{jp} + b_{jp} \sigma_{ip}). \quad (8)$$

If there were no uncertainties, then the  $\sigma_{pq}$  in eq (7) would be zero, there would be no need for eq (8), and eq (7) reduces to eq (2).

Solving eq (7) and (8) requires knowledge concerning the third moments about the mean. One can derive an equation for the third moments (cf. Fleming 1970), but it involves fourth moments. The complete stochastic dynamic equations form an infinite unclosed set of coupled equations. The equations are thus unsolvable until an algorithm is devised to close the set. The algorithm or closure scheme chosen by Epstein was just to drop the third moment terms in eq (8). The implications of this technique and other closure methods are discussed below where the closure problem is studied more fully. It will be mentioned here, though, that even if the third moments of the ensemble are initially zero (for example, the variables are multivariate normally distributed initially) they will not remain zero. The time required for the third moments to grow and the extent to which they will grow, thus alter-

ing the results of the truncated system of equations, is the fundamental question to be answered.

### 3. APPLICATION TO A BAROCLINIC SYSTEM

Epstein (1969b) used a simple barotropic model of the atmosphere for his stochastic dynamic equations. In a barotropic atmosphere, there is no change of wind with height so that the atmosphere can be characterized by a single level. Since the early days of numerical forecasting, the barotropic model has been used to forecast the 500-mb level of the atmosphere. In such a model, the only energy exchange that can take place is between the kinetic energy of the eddies and the kinetic energy of the zonal flow. Thus, it is the next logical step to use a more complex model of the atmosphere for the stochastic dynamic equations. On the other hand, there are many fundamental questions to be answered concerning the dynamics and energetics of an ensemble in phase space, so that it is desirable to keep the model simple enough to isolate the answers to these questions.

A model which ideally suits the purpose here was used by Lorenz (1963b) to study different regimes of flow. This model was extended by increasing the spectral resolution (Lorenz 1965) in a study of predictability. The extended model transforms the space domain into orthogonal functions which describe three different wave numbers in the  $x$ -direction and two orthogonal modes in the  $y$ -direction. ("Mode" refers to the  $y$ -variation.) This model is the basic model used in this study. It is also extended to include 15 different waves in the  $x$ -direction for a predictability study to be described in part II.

The details and equations of this two-level model were developed by Lorenz (1960, 1963b, 1965) and are only stated here. The basic equations are the quasi-geostrophic vorticity equation and the thermal equation, that can be written with  $x, y$  as horizontal coordinates and pressure,  $p$ , as the vertical coordinate. The equations for the model written in spectral form are

$$\dot{\psi}_i = \sum_{j,k=1}^{\infty} [a_i^{-2} (a_j^2 - a_k^2) C_{ijk} (\psi_j \psi_k + \theta_j \theta_k)] - \kappa (\psi_i - \theta_i) \quad (9)$$

and

$$\dot{\theta}_i = \sum_{j,k=1}^{\infty} \left[ C_{ijk} \frac{\sigma_0 (a_j^2 - a_k^2) + 1}{\sigma_0 a_i^2 + 1} \theta_j \psi_k + C_{ijk} \frac{\sigma_0 (a_j^2 - a_k^2) - 1}{\sigma_0 a_i^2 + 1} \psi_j \theta_k \right] + \frac{\kappa \sigma_0 a_i^2}{\sigma_0 a_i^2 + 1} \psi_i - \frac{\sigma_0 a_i^2 (\kappa + 2\kappa') + h}{\sigma_0 a_i^2 + 1} \theta_i + \frac{h}{\sigma_0 a_i^2 + 1} \theta_i^* \quad (10)$$

where  $\psi$  and  $\theta$  are nondimensional dependent variables representing the mean wind and mean potential temperature;  $\kappa, \kappa', h, \sigma$ , and the  $\theta_i^*$  (all described below) are nondimensional constants;  $a_i$  and  $C_{ijk}$  are constants depending upon the choice of the orthogonal functions  $F_i$  used to represent the space domain (described below). Quantities have been made dimensionless by appropriate scale factors including a length  $L$  and a time  $f^{-1}$  ( $f$  is the Coriolis parameter assumed constant in this case). The dot in eq (9) and (10) denotes differentiation with respect to the dimensionless time.

A simple two-layer model like this is incapable of describing the complicated boundary-layer physics of the real atmosphere. Therefore, it is necessary to parameterize the boundary-layer effects by the use of coefficients of heating and friction. A frictional drag with coefficient  $2\kappa$  is introduced at the lower surface, proportional to the velocity in the lower layer. A frictional drag at the boundary separating the two layers with coefficient  $\kappa'$  is introduced, proportional to the shear at this surface. There is a heating of the lower layer, proportional to the difference between the temperature of the lower layer and a pre-assigned temperature field  $\theta^*$ , characterized by a coefficient  $2h$ . A coefficient for heat exchange between the layers cancels out when  $\sigma$  (a measure of static stability) is considered constant as discussed below.

In his application of this model to a consideration of predictability, Lorenz (1965) considered  $\sigma$  as a constant in space and time. This assumption concerning  $\sigma$  is used here, so that predictability results can be compared to those of Lorenz. If  $\sigma$  is a function of pressure, as in the real atmosphere, this leads to products of three variables—which, in turn, means that at least some third moments must be retained. If the model was “primitive” instead of quasi-geostrophic, the equations would contain no triple products.

To solve these equations, we must determine the values of  $a_i$  and  $C_{ijk}$ . These values are determined by the chosen set of orthogonal functions  $F_i$ . The choice of the functions depends upon the geometry of the space domain in which the model equations are applied. Following Lorenz (1965), these functions are given over an infinite channel of width  $\pi L$  having walls at the surfaces  $y=0$  and  $y=\pi L$ , where the flow in the channel is periodic along the length, with a specified fundamental wavelength. The functions are

$$\begin{aligned}\Phi_{00} &= 1, \\ \Phi_{0m} &= \sqrt{2} \cos my/L & m=1, 2, \\ \Phi_{nm} &= 2 \cos(nax/L) \sin my/L \\ & \quad m=1, 2; \quad n=1, 2, 3, \\ \text{and} \quad \Phi'_{nm} &= 2 \sin(nax/L) \sin my/L \\ & \quad m=1, 2; \quad n=1, 2, 3\end{aligned}\quad (11)$$

where  $a$  is an integer chosen to specify the ratio of the fundamental wavelength in the  $x$ -direction.

It is readily verified that these functions are indeed orthogonal. For clarification in deriving the energy relationships for the stochastic dynamic form of the above deterministic spectral equations, the following notation is adopted for the 14 functions:

$$\begin{aligned}\Phi_{(1)} &= \sqrt{2} \cos y/L, \\ \Phi_{(2,3,4)} &= 2 \cos[(a, 2a, 3a)x/L] \sin y/L, \\ \Phi_{(5,6,7)} &= 2 \sin[(a, 2a, 3a)x/L] \sin y/L, \\ \Phi_{(8)} &= \sqrt{2} \cos 2y/L, \\ \Phi_{(9,10,11)} &= 2 \cos[(a, 2a, 3a)x/L] \sin 2y/L, \\ \text{and} \quad \Phi_{(12,13,14)} &= 2 \sin[(a, 2a, 3a)x/L] \sin 2y/L.\end{aligned}\quad (12)$$

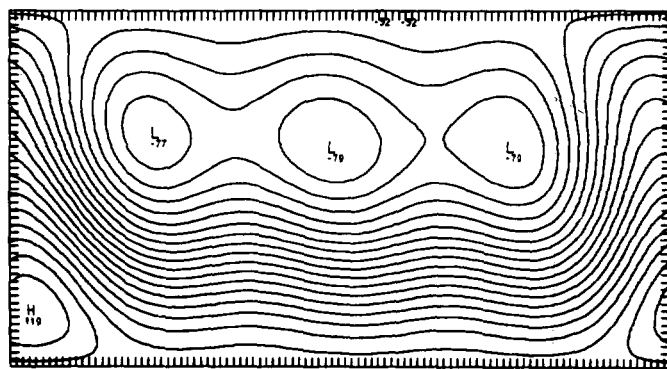


FIGURE 2.—Initial stream field  $\psi$  for deterministic and stochastic dynamic methods.

Note that functions 1 through 7 represent mode 1, and 8 through 14 refer to mode 2. The zonal components of the flow are functions 1 and 8; the eddy components are all the other functions.

The method of obtaining the  $a_i^2$  and  $C_{ijk}$  is given by Lorenz (1963b) and their values are given by Fleming (1970). There are certain “selection” rules that admit desired sets of pairs of functions for the nonlinear term on the right side of the spectral equations; these pairs of functions are those which interact with the third function on the left of the spectral equation. For the 28-variable model (14 orthogonal functions for  $\psi$  and  $\theta$ ), the different pairs which interact with each of the respective functions are determined from the “selection” rules and stored in tables.

The physics of the model to be used can be conveniently summarized. The quasi-geostrophic equations have been used to describe thermally forced rotating flow in the domain of the infinite channel. Sound and gravity waves have been filtered from the solutions by the hydrostatic and geostrophic equations. The transport of momentum by the vertical motions and by the divergent part of the horizontal motions has been left out of the vorticity equation. However, the transport of heat by the total horizontal and vertical motions is present because no such assumptions were made in the thermal equations. Flow in the model is slowed by internal and surface friction. There is no vertical velocity at the top and bottom of the model, and no exchange of heat and momentum through the sides of the channel.

In all the calculations in this study, the finite difference scheme used for the time derivative in eq (9) and (10) is the fourth-order Kutta-Simpson method which is described in many texts (e.g., Hildebrand 1965).

An example of the results of a deterministic and stochastic dynamic forecast with the model is given below. The initial stream field for both methods is shown in figure 2. The linear and constant terms have been set to zero which means the model is now adiabatic and frictionless. The mean values of  $\psi_i$  and  $\theta_i$  are the same as the  $\psi_i$  and  $\theta_i$  for the deterministic forecast. The ensemble members are normally distributed about the mean for the stochastic model. The variables have a standard deviation

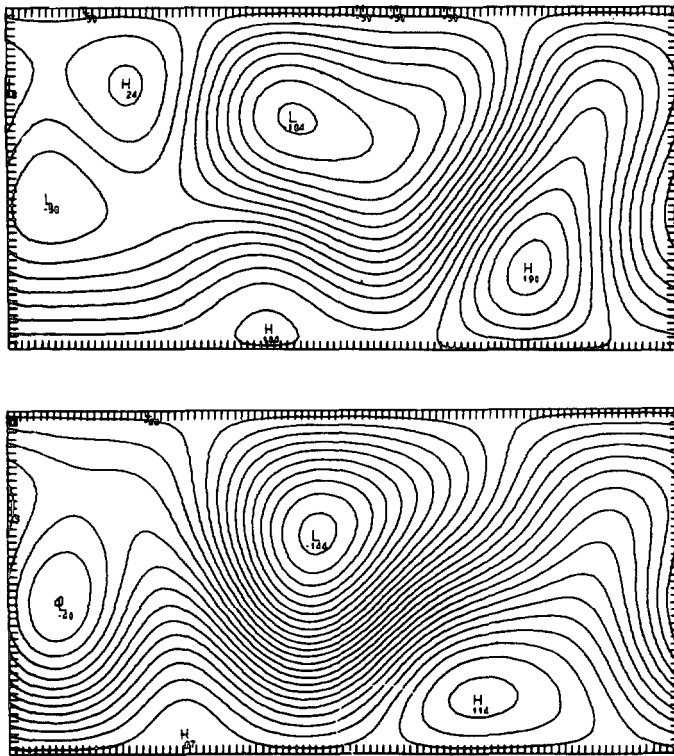


FIGURE 3.—Stream field after 7 days for deterministic (top) and stochastic dynamic (bottom) cases. The contour intervals are not the same.

of 10 percent of the mean, but the initial variables are uncorrelated—all covariances are zero. The results after one week are shown in figure 3. We see that the deterministic forecast differs from the ensemble mean forecast. The features differ in intensity, position, and shape. As pointed out by Epstein (1969b), this does not mean the deterministic forecast is wrong, as it is possible that the deterministic solution would verify since it is a member of the ensemble. The stochastic solution represents the ensemble mean and stochastic solutions will be more representative since they have been designed to minimize mean square error based upon all the sources of uncertainty.

It will be seen in later figures presented in this paper that, with small uncertainties confined to the initial conditions, the deterministic forecasts of the variables and the stochastic forecasts of their means will be essentially alike in the *early* stages of the time integration. However, the advantage of the stochastic equations is the additional knowledge given about the uncertainties of these variables and about how they are dynamically coupled.

#### 4. ENERGETICS OF UNCERTAINTY

The results shown in the preceding section are similar to those of Epstein (1969b). They give rise to certain questions. How does the uncertainty grow? Why are some physical situations more prone to error growth than others?

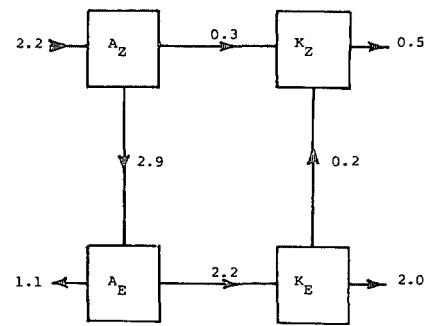


FIGURE 4.—Quasi-geostrophic energy diagram. Values from Wiin-Nielsen (1968).

What fundamentally determines the evolution of the hypothetical ensemble of points in phase space? An attempt will be made to gain insight into the answers to these questions by viewing the energy processes. It is realized that *complete* answers would depend upon *analytical* solutions of the original nonlinear deterministic set of equations which, of course, are not available.

Many authors have contributed to the understanding of the atmosphere by considering the energetics of the deterministic equations. The intent here is to give a brief summary of the basic energy concepts. This will provide a foundation upon which to build the concepts of the energetics of uncertainty.

There are three significant forms of energy in the atmosphere: internal, potential, and kinetic. In a hydrostatic atmosphere, the internal and potential energy are proportional and are conveniently combined to form the "total potential energy." In dealing with the exchanges between these types of energy, Lorenz (1955) found it convenient to define the "available potential energy" as that portion of the total potential energy which may be available for conversion into kinetic energy. Lorenz also derives an approximate expression for available potential energy which has since been shown to be energetically consistent with the quasi-geostrophic equations (cf. Wiin-Nielsen 1968). Representative values of the generation, conversion, and dissipation of energy obtained from the quasi-geostrophic calculations are given by Wiin-Nielsen (1965, 1968). His values, shown in figure 4, do not reflect the effects of the Tropics. In this figure,  $A$  and  $K$  refer to available potential and kinetic energy; the subscripts  $Z$  and  $E$  refer to zonal and eddy components of the energy,  $G(X)$  refers to a generation of  $X$ ,  $D(X)$  refers to a dissipation of  $X$ ,  $C(X,Y)$  refers to a conversion of  $X$  into  $Y$ . The conversion  $C(A_Z, K_Z)$  is taken from Dutton and Johnson (1967).

A positive generation will occur when there is diabatic heating where it is warm and cooling where it is cold. The dissipation of kinetic energy is due to friction effects in the boundary layer and internal friction within the atmosphere. The conversion  $C(A_Z, A_E)$  depends upon transporting heat from a warm latitude to a cold latitude, and

alternately, the transport of cooler air from a cold latitude to a warm one. The conversion  $C(K_E, K_Z)$  depends upon whether the transport of angular momentum is toward latitudes of higher or lower angular velocity. The conversions  $C(A, K)$  are positive when warm air is rising and cold air is sinking.

A more complete derivation of the stochastic dynamic energy relationships obtained from the stochastic dynamic model is given below, but all those deterministic energy relationships will be used without derivation. The baroclinic stochastic dynamic equations and their energetics will yield, for the first time, substantial insight into why and by how much a deterministic forecast may differ from the real atmosphere

## 5. DERIVATION OF ENERGY EQUATIONS

In the absence of heating and friction, the condition  $\sum_i a_{ipq} X_i X_p X_q = 0$  on eq (2) implies that  $\sum_i X_i^2$  is conserved (cf. Lorenz 1963a). The corresponding adiabatic frictionless model [given by eq (9) and (10) with the linear and constant terms set equal to zero] conserves the quantity  $(K+A)$  where  $K$  is kinetic energy and  $A$  is Lorenz' approximated available potential energy. It is easily verified that

$$K = \frac{s}{2} \sum_i a_i^2 (\psi_i^2 + \theta_i^2) \quad (13)$$

and

$$A = \frac{s}{2\sigma_0} \sum_i \theta_i^2 \quad (14)$$

where  $s$  is a scale factor given by  $P_0 L^2 f^2 / g$  ( $g$  is the acceleration of gravity). In the remainder of this paper, the scale factor will be ignored and  $\sigma_0$  will be referred to as  $\sigma$ .

The stochastic equations applied to the general expression, eq (2), reveal that the quantity  $\sum_i (\mu_i^2 + \sigma_{ii})$  is conserved. Denoting the conserved quadratic quantities as energy (they could represent enstrophy—mean squared vorticity) reveals that the stochastic dynamic equations provide for a partitioning of the energy as pointed out by Epstein (1969b). There is "certain" energy associated with the expected components of the ensemble and "uncertain" energy associated with the variances. The uncertain energy cannot be "specified" (e.g., as to location) within the model.

The initial uncertain energy may represent, in part, some of the actual energy of the atmosphere; that is, it may be energy lost by smoothing the data, or turbulent energy, or any small-scale energy unresolved by the deterministic initial conditions. (In the statistical approach to analytical theories of turbulence, these variances are referred to as the "turbulent" energy.) However, the variances (whatever name they be given) are a direct measure of the growth of uncertainty in the values of the variables. The names used here are especially appropriate in that the growth of uncertainty will be seen to depend

upon the dynamic coupling between the variables, and the energy exchange processes associated with these couplings.

The stochastic dynamic equations applied to the deterministic equations for the two-level model, eq (9) and (10), give the following result:

$$K = \sum_i \frac{a_i^2}{2} [\psi_i^2 + \theta_i^2 + \text{var}(\psi_i) + \text{var}(\theta_i)] \quad (15)$$

and

$$A = \sum_i \frac{1}{2\sigma} [\theta_i^2 + \text{var}(\theta_i)] \quad (16)$$

where var is variance. The quantity

$$\sum_i \frac{a_i^2}{2} (\psi_i^2 + \theta_i^2)$$

is the certain kinetic energy;

$$\sum_i \frac{a_i^2}{2} [\text{var}(\psi_i) + \text{var}(\theta_i)]$$

is the uncertain kinetic energy;

$$\sum_i \theta_i^2 / 2\sigma$$

is the certain available potential energy; and

$$\sum_i \frac{\text{var}(\theta_i)}{2\sigma}$$

is the uncertain available potential energy.

The quantities  $\psi_i$  and  $\theta_i$  in the above equations now refer to the mean values of  $\psi_i$  and  $\theta_i$  in the stochastic dynamic model, whereas the same symbols have been used for the deterministic stream function and potential temperature. There will be no confusion, as only the stochastic dynamic equations will be referred to in the remainder of this paper.

Taking the time derivative of eq (15) and (16) gives

$$\begin{aligned} \dot{K} = & \sum_i a_i^2 \dot{\psi}_i \dot{\psi}_i + \sum_i a_i^2 \dot{\theta}_i \dot{\theta}_i \\ & + \sum_i \frac{a_i^2}{2} [\dot{\text{var}}(\psi_i)] + \sum_i \frac{a_i^2}{2} [\dot{\text{var}}(\theta_i)] \end{aligned} \quad (17)$$

and

$$\dot{A} = \sum_i \frac{\dot{\theta}_i \dot{\theta}_i}{\sigma} + \sum_i \frac{[\dot{\text{var}}(\theta_i)]}{2\sigma} \quad (18)$$

The zonal component of either energy includes the terms for which  $i=1$  and 8. The eddy component is computed by summing the terms over  $i=2, 3, \dots, 14$ ;  $i \neq 8$ . Thus, expressions for  $\dot{A}_Z$ ,  $\dot{K}_Z$ ,  $\dot{A}_E$ ,  $\dot{K}_E$  and their uncertain counterparts  $U\dot{A}_Z$ ,  $U\dot{K}_Z$ ,  $U\dot{A}_E$ ,  $U\dot{K}_E$  can be obtained from the expressions for  $\dot{\psi}_i$ ,  $\dot{\theta}_i$ ,  $[\dot{\text{var}}(\psi_i)]$ , and  $[\dot{\text{var}}(\theta_i)]$ . By comparing the terms on the right-hand side of the equations for



the time derivatives of the various energy quantities, the exact energy relationships that exist between the quantities can be determined. Although this is a tedious manipulation, a procedure is given here since the energy relations which result are quite important. Instead of writing time derivatives of the eight different energy quantities, much space can be saved by "selectively" grouping terms and showing that the "grouped" terms are the indicated energy conversions.

The restriction of adiabatic frictionless flow is removed and the complete equations for  $\dot{\psi}_i$ ,  $\dot{\theta}_i$ ,  $[\text{var}(\psi_i)]$ , and  $[\text{var}(\theta_i)]$  are

$$\dot{\psi}_i = AM_i + AMQ_i - CM_i \quad (19)$$

$$\dot{\theta}_i = \sigma AS_i + B_i + \sigma CS_i - \sigma D_i + F_i - E_i + \sigma ASQ_i + BQ_i, \quad (20)$$

$$[\text{var}(\psi_i)] = 2AMU_i - 2CMU_i, \quad (21)$$

and

$$[\text{var}(\theta_i)] = 2\sigma ASU_i + 2BU_i + 2\sigma CSU_i - 2\sigma DU_i - 2EU_i \quad (22)$$

where

$$\begin{aligned} AM_i &= \sum a_i^{-2} (a_k^2 - a_l^2) C_{ikl} (\psi_k \psi_l + \theta_k \theta_l), \\ AS_i &= \sum \left( \frac{1}{\sigma a_i^2 + 1} \right) C_{ikl} (a_k^2 - a_l^2) (\theta_k \psi_l + \psi_k \theta_l), \\ B_i &= \sum \frac{C_{ikl}}{\sigma a_i^2 + 1} (\theta_k \psi_l - \psi_k \theta_l), \\ CM_i &= \kappa (\psi_i - \theta_i), \\ CS_i &= \left( \frac{1}{\sigma a_i^2 + 1} \right) a_i^2 \kappa \psi_i, \\ D_i &= \left( \frac{1}{\sigma a_i^2 + 1} \right) a_i^2 (\kappa + 2\kappa') \theta_i, \\ E_i &= \left( \frac{h}{\sigma a_i^2 + 1} \right) \theta_i, \end{aligned}$$

and

$$F_i = \left( \frac{h}{\sigma a_i^2 + 1} \right) \theta_i^* \quad (23)$$

refer to terms coming from first moments and eventually define certain energy relations, and  $M$  or  $S$  refers to a term's source as being from the mean flow equation or the shear flow equation. The terms that come from second moments about the mean are

$$\begin{aligned} AMQ_i &= \sum a_i^{-2} (a_k^2 - a_l^2) C_{ikl} [\text{cov}(\psi_k, \psi_l) + \text{cov}(\theta_k, \theta_l)], \\ ASQ_i &= \sum \left( \frac{1}{\sigma a_i^2 + 1} \right) C_{ikl} (a_k^2 - a_l^2) [\text{cov}(\theta_k, \psi_l) + \text{cov}(\psi_k, \theta_l)], \\ BQ_i &= \sum \frac{C_{ikl}}{\sigma a_i^2 + 1} [\text{cov}(\theta_k, \psi_l) - \text{cov}(\psi_k, \theta_l)] \end{aligned} \quad (24)$$

where  $Q$  refers to terms that eventually define or link "certain" energy relations;  $\text{cov}$  is covariance; and

$$\begin{aligned} AMU_i &= \sum a_i^{-2} (a_k^2 - a_l^2) C_{ikl} [\psi_k \text{cov}(\psi_i, \psi_l) \\ &\quad + \psi_i \text{cov}(\psi_l, \psi_k) + \theta_k \text{cov}(\psi_i, \theta_l) + \theta_l \text{cov}(\psi_i, \theta_k)], \\ ASU_i &= \sum \left( \frac{1}{\sigma a_i^2 + 1} \right) C_{ikl} (a_k^2 - a_l^2) [\theta_k \text{cov}(\theta_i, \psi_l) \\ &\quad + \psi_i \text{cov}(\theta_l, \theta_k) + \psi_k \text{cov}(\theta_l, \theta_i) + \theta_l \text{cov}(\theta_i, \psi_k)], \\ BU_i &= \sum \frac{C_{ikl}}{\sigma a_i^2 + 1} [\theta_k \text{cov}(\theta_i, \psi_l) + \psi_i \text{cov}(\theta_l, \theta_k) \\ &\quad - \psi_k \text{cov}(\theta_l, \theta_i) - \theta_l \text{cov}(\theta_i, \psi_k)], \\ CMU_i &= \kappa [\text{var}(\psi_i) - \text{cov}(\psi_i, \theta_i)], \\ CSU_i &= \frac{1}{\sigma a_i^2 + 1} a_i^2 \kappa \text{cov}(\theta_i, \psi_i), \\ DU_i &= \frac{1}{\sigma a_i^2 + 1} a_i^2 (\kappa + 2\kappa') \text{var}(\theta_i), \text{ and} \\ EU_i &= \frac{h}{\sigma a_i^2 + 1} \text{var}(\theta_i) \end{aligned} \quad (25)$$

where  $U$  refers to terms that eventually define uncertain energy relations.

The summation sign in the above definitions implies a double summation over  $k$  and  $l$  with  $l > k$ . Substituting eq (19) through (22) into the equations for the time rate of change of kinetic and available potential energy given by eq (17) and (18) results in energy change equations that are completely expressed with terms that are known at any given instant of time. The resulting equations are

$$\begin{aligned} \dot{K} &= \sum_i [a_i^2 \psi_i (AM_i + AMQ_i - CM_i) + a_i^2 \theta_i (\sigma AS_i + B_i + \sigma CS_i \\ &\quad - \sigma D_i + F_i - E_i + \sigma ASQ_i + BQ_i) + a_i^2 (AMU_i - CMU_i) \\ &\quad + a_i^2 (\sigma ASU_i + BU_i + \sigma CSU_i - \sigma DU_i - EU_i)] \end{aligned} \quad (26)$$

and

$$\begin{aligned} \dot{A} &= \sum_i [\theta_i (AS_i + B_i/\sigma + CS_i - D_i + F_i/\sigma - E_i/\sigma \\ &\quad + ASQ_i + BQ_i/\sigma) + (ASU_i + BU_i/\sigma + CSU_i - DU_i - EU_i/\sigma)]. \end{aligned} \quad (27)$$

Selectively regrouping terms gives

$$\begin{aligned} \dot{K} &= \sum_i \{ -[\theta_i \omega'_i]_1 - [\omega'_i]_2 - [a_i^2 \psi_i CM_i \\ &\quad - (1 + a_i^2 \sigma) \theta_i (CS_i - D_i)]_3 - [a_i^2 CMU_i - (1 + a_i^2 \sigma) (CSU_i \\ &\quad - DU_i)]_4 + [a_i^2 \psi_i AM_i + (1 + a_i^2 \sigma) \theta_i AS_i]_5 + [a_i^2 \psi_i AMQ_i \\ &\quad + (1 + a_i^2 \sigma) \theta_i ASQ_i + a_i^2 AMU_i + (1 + a_i^2 \sigma) ASU_i]_6 \} \end{aligned} \quad (28)$$

and

$$\begin{aligned} \dot{A} &= \sum_i \left\{ [\theta_i \omega'_i]_1 + [\omega'_i]_2 + \left[ \theta_i \left( \frac{a_i^2 \sigma + 1}{\sigma} \right) (F_i - E_i) \right]_7 \right. \\ &\quad - \left[ \left( \frac{a_i^2 \sigma + 1}{\sigma} \right) EU_i \right]_8 + \left[ \theta_i \left( \frac{a_i^2 \sigma + 1}{\sigma} \right) B_i \right]_9 \\ &\quad \left. + \left[ \theta_i \left( \frac{a_i^2 \sigma + 1}{\sigma} \right) BQ_i + \left( \frac{a_i^2 \sigma + 1}{\sigma} \right) BU_i \right]_{10} \right\} \end{aligned} \quad (29)$$



where

$$\omega'_i = AS_i + ASQ_i - a_i^2(B_i + BQ_i) + CS_i - D_i - a_i^2(F_i - E_i), \quad (30)$$

$$\omega''_i = ASU_i - a_i^2BU_i + CSU_i - DU_i + a_i^2EU_i, \quad (31)$$

and the numbered brackets serve only to identify terms. Equations (28) and (29) can be made dimensional by multiplying each term by the scale factor  $(P_0 L^2 f^3 / g)$ .

It can be shown that  $\omega'_i$  corresponds exactly to the expected value of vertical velocity in pressure coordinates at the surface between the layers. Thus, the bracketed terms "1", that appear in eq (28) and (29) with opposite sign, agree with the definition of  $C(A, K)$  from quasi-geostrophic theory. The conversions for the certain  $A$  to  $K$  are then given by

$$C(A_z, K_z) = -\sum_i \theta_i \omega'_i \quad i=1 \text{ and } 8 \quad (32)$$

and

$$C(A_E, K_E) = -\sum_i \theta_i \omega'_i \quad i=2, 3, \dots, 14; i \neq 8. \quad (33)$$

The conversions for the uncertain  $A$  to  $K$  are similarly given by terms "2":

$$C(UA_z, UK_z) = -\sum_i \omega''_i \quad i=1 \text{ and } 8 \quad (34)$$

$$C(UA_E, UK_E) = -\sum_i \omega''_i \quad i=2, 3, \dots, 14; i \neq 8. \quad (35)$$

The generation of available potential energy is proportional to the correlation of heating and temperature. In eq (29), since all the heating effect is contained in  $E_i$  and  $F_i$ , the certain generation is given by terms "7" and the uncertain generation by term "8". These generations are more clearly identified at the end of this section where the notation is replaced and the complete energy equations are summarized.

Since all the friction effects are in  $CM_i$ ,  $CS_i$ , and  $D_i$ , the certain and uncertain dissipation of kinetic energy is given in eq (28) by the terms "3" and "4", respectively.

The conversion  $C(A_z, A_E)$  is given by the negative of term "9" in eq (29). This is not as immediately evident as the other conversions so a proof is given below. Since the spectral equations used here completely describe each triplet of wave vectors capable of interacting down to some truncated scale, only one of the triplets need be considered for this proof. Consider the triplet  $(i, k, l)$  where  $i$  is a zonal function and  $k$  and  $l$  are eddy functions. Equation (29), considering *only* term "9", gives

$$\dot{A}_z = \frac{C_{ikl}}{\sigma} \theta_i (\theta_k \psi_l - \psi_k \theta_l) + \dots \quad (36)$$

and for the eddies.

$$\dot{A}_E = \frac{1}{\sigma} [C_{kli} (\theta_k \psi_l - \psi_l \theta_i) + \theta_i C_{lik} (\theta_k \psi_l - \psi_l \theta_k)] + \dots \quad (37)$$

Since  $C_{ikl} = C_{kli} = C_{lik}$ , eq (37) can be written

$$\dot{A}_E = \frac{1}{\sigma} [C_{ikl} (\theta_k \theta_i \psi_l - \theta_k \psi_l \theta_i + \theta_i \theta_k \psi_l - \theta_k \psi_l \theta_i)] + \dots \quad (38)$$

or

$$\dot{A}_E = -\frac{C_{ikl}}{\sigma} (\theta_k \psi_l - \psi_k \theta_l) \theta_i + \dots \quad (39)$$

Thus, the first term on the right of eq (39) is equal and opposite in sign to that of eq (36). This also implies that the sum of all the components in term "9" is identically zero.

We have shown that term "9" gives  $C(A_E, A_z)$ , or that the negative of term "9" gives  $C(A_z, A_E)$ . By the same method used above, it can be easily verified that  $C(K_E, K_z)$  is given by term "5" of eq (28).

In much the same manner as above, the conversions  $C(UA_z, UA_E)$ ,  $C(UA_E, A_z)$ ,  $C(A_E, UA_z)$ , and  $C(A_E, UA_E)$  can be obtained from term "10" in eq (29). The proof of these conversions is given by Fleming (1970). The method involves considering the "zonal-eddy" triplets and all distinct "eddy-only" triplets. Many terms are involved that must be "tagged" as to their source, but the procedure is the same as above.

The remaining energy conversions  $C(UK_E, UK_z)$ ,  $C(UK_E, K_z)$ ,  $C(K_E, UK_z)$ , and  $C(K_E, UK_E)$  are obtained from term "6" of eq (28) just as described in the preceding paragraph. A complete summary of the certain and uncertain energy generation, conversion, and dissipation equations is given below.

$$G(A_z) = \sum_i \frac{h}{\sigma} \theta_i (\theta_i^* - \theta_i) \quad i=1, 8, \quad (40)$$

$$G(A_E) = \sum_i \frac{h}{\sigma} \theta_i (\theta_i^* - \theta_i) \quad i=2, 3, \dots, 14; i \neq 8, \quad (41)$$

$$D(K_z) = \sum_i a_i^2 \kappa [\psi_i^2 - 2\psi_i \theta_i + \theta_i^2] + a_i^2 (2\kappa') \theta_i^2 \quad i=1, 8, \quad (42)$$

$$D(K_E) = \sum_i a_i^2 \kappa [\psi_i^2 - 2\psi_i \theta_i + \theta_i^2] + a_i^2 (2\kappa') \theta_i^2 \quad i=2, 3, \dots, 14; i \neq 8, \quad (43)$$

$$C(A_z, A_E) = \sum_i \sum_{k,l} \frac{\theta_i}{\sigma} C_{ikl} (\theta_k \psi_l - \psi_k \theta_l) \quad i=1, 8, \quad (44)$$

$$C(K_E, K_z) = \sum_i \sum_{k,l} (a_k^2 - a_l^2) C_{ikl} [\psi_i (\psi_k \psi_l + \theta_k \theta_l) + \theta_i (\theta_k \psi_l + \psi_k \theta_l)] \quad i=1, 8, \quad (45)$$

$$C(A_z, K_z) = -\sum_i \omega'_i \theta_i \quad i=1, 8, \quad (46)$$

$$C(A_E, K_E) = -\sum_i \omega'_i \theta_i \quad i=2, 3, \dots, 14; i \neq 8, \quad (47)$$

$$G(UA_z) = -\sum_i \frac{h}{\sigma} \text{var}(\theta_i) \quad i=1, 8, \quad (48)$$

$$G(UA_E) = -\sum_i \frac{h}{\sigma} \text{var}(\theta_i) \quad i=2,3, \dots, 14; i \neq 8, \quad (49)$$

$$D(UK_Z) = \sum_i a_i^2 \kappa [\text{var}(\psi_i) - 2 \text{cov}(\psi_i, \theta_i) + \text{var}(\theta_i)] + a_i^2 (2\kappa') \text{var}(\theta_i) \quad i=1,8, \quad (50)$$

$$D(UK_E) = \sum_i a_i^2 \kappa [\text{var}(\psi_i) - 2 \text{cov}(\psi_i, \theta_i) + \text{var}(\theta_i)] + a_i^2 (2\kappa') \text{var}(\theta_i) \quad i=2,3, \dots, 14; i \neq 8, \quad (51)$$

$$C(UA_Z, UA_E) = \sum_i \sum_{k,l} \frac{C_{ikl}}{\sigma} [\psi_k \text{cov}(\theta_i, \theta_l) - \psi_l \text{cov}(\theta_i, \theta_k)] \quad i=1,8, \quad (52)$$

$$C(UK_E, UK_Z) = \sum_i \sum_{k,l} a_k^2 C_{ikl} \{ \theta_k [\text{cov}(\psi_i, \theta_l) + \text{cov}(\theta_i, \psi_l)] + \psi_k [\text{cov}(\psi_i, \psi_l) + \text{cov}(\theta_i, \theta_l)] \} - a_i^2 C_{ikl} \times \{ \theta_l [\text{cov}(\psi_i, \theta_k) + \text{cov}(\theta_i, \psi_k)] + \psi_l [\text{cov}(\psi_i, \psi_k) + \text{cov}(\theta_i, \theta_k)] \} \quad i=1,8, \quad (53)$$

$$C(UA_Z, UK_Z) = -\sum_i \omega_i'' \quad i=1,8, \quad (54)$$

$$C(UA_E, UK_E) = -\sum_i \omega_i'' \quad i=2,3, \dots, 14; i \neq 8, \quad (55)$$

$$C(A_Z, UA_E) = \sum_i \sum_{k,l} \frac{C_{ikl}}{\sigma} \{ \theta_i [\text{cov}(\psi_k, \theta_l) - \text{cov}(\theta_k, \psi_l)] \} \quad i=1,8, \quad (56)$$

$$C(A_E, UA_Z) = \sum_i \sum_{k,l} \frac{C_{ikl}}{\sigma} [\theta_k \text{cov}(\theta_i, \psi_l) - \theta_l \text{cov}(\theta_i, \psi_k)] \quad i=1,8, \quad (57)$$

$$C(A_E, UA_E) = \sum_{i=1,8} \sum_{k,l} \frac{C_{ikl}}{\sigma} [\theta_l \text{cov}(\theta_k, \psi_i) - \theta_k \text{cov}(\theta_l, \psi_i)] + \sum_{\substack{\text{"distinct"} \\ \text{triplets} \\ i < k \text{ or } l}} \left[ \frac{C_{ikl}}{\sigma} \{ \theta_i [\text{cov}(\psi_k, \theta_l) - \text{cov}(\theta_k, \psi_l)] + \theta_k [\text{cov}(\psi_i, \theta_l) - \text{cov}(\theta_l, \psi_i)] + \theta_l [\text{cov}(\psi_i, \theta_k) - \text{cov}(\theta_i, \psi_k)] \} \right], \quad (58)$$

$$C(K_Z, UK_E) = -\sum_i \sum_{k,l} (a_k^2 - a_l^2) C_{ikl} \{ \theta_i [\text{cov}(\theta_k, \psi_l) + \text{cov}(\psi_k, \theta_l)] + \psi_i [\text{cov}(\psi_k, \psi_l) + \text{cov}(\theta_k, \theta_l)] \} \quad i=1,8, \quad (59)$$

$$C(K_E, UK_Z) = \sum_i \sum_{k,l} (a_k^2) C_{ikl} \{ \theta_i [\text{cov}(\psi_i, \theta_k) + \text{cov}(\theta_i, \psi_k)] + \psi_i [\text{cov}(\psi_i, \psi_k) + \text{cov}(\theta_i, \theta_k)] \} - (a_i^2) C_{ikl} \times \{ \theta_k [\text{cov}(\psi_i, \theta_l) + \text{cov}(\theta_l, \psi_i)] + \psi_k [\text{cov}(\psi_i, \psi_l) + \text{cov}(\theta_l, \theta_i)] \} \quad i=1,8, \quad (60)$$

and

$$C(K_E, UK_E) = \sum_{i=1,8} \sum_{k,l} (a_i^2) C_{ikl} \{ \theta_k [\text{cov}(\psi_i, \theta_l) + \text{cov}(\theta_i, \psi_l)] + \psi_k [\text{cov}(\psi_i, \psi_l) + \text{cov}(\theta_i, \theta_l)] - \theta_l [\text{cov}(\psi_i, \theta_k) + \text{cov}(\theta_l, \psi_k)] - \psi_l [\text{cov}(\psi_i, \psi_k) + \text{cov}(\theta_l, \theta_k)] \} + \sum_{\substack{\text{"distinct"} \\ \text{triplets} \\ i < k \text{ or } l}} C_{ikl} \left[ (a_k^2) \{ \theta_l [\text{cov}(\theta_i, \psi_k) + \text{cov}(\psi_i, \theta_k)] + \psi_l [\text{cov}(\psi_i, \psi_k) + \text{cov}(\theta_i, \theta_k)] - \theta_i [\text{cov}(\theta_k, \psi_l) + \text{cov}(\psi_k, \theta_l)] - \psi_i [\text{cov}(\psi_k, \psi_l) + \text{cov}(\theta_k, \theta_l)] + (a_l^2) \{ \theta_i [\text{cov}(\theta_k, \psi_l) + \text{cov}(\psi_k, \theta_l)] + \psi_i [\text{cov}(\psi_k, \psi_l) + \text{cov}(\theta_k, \theta_l)] - \theta_k [\text{cov}(\theta_i, \psi_l) + \text{cov}(\psi_l, \theta_i)] - \psi_k [\text{cov}(\psi_i, \psi_l) + \text{cov}(\theta_i, \theta_l)] + (a_i^2) \{ \theta_k [\text{cov}(\theta_l, \psi_i) + \text{cov}(\psi_l, \theta_i)] + \psi_k [\text{cov}(\psi_l, \psi_i) + \text{cov}(\theta_l, \theta_i)] - \theta_l [\text{cov}(\theta_i, \psi_k) + \text{cov}(\psi_i, \theta_k)] - \psi_l [\text{cov}(\psi_i, \psi_k) + \text{cov}(\theta_i, \theta_k)] \} \right]. \quad (61)$$

The energy generations, conversions, and dissipations of the baroclinic stochastic dynamic model are indicated in an energy diagram shown in figure 5. The energy equations would be the same for any number of orthogonal functions, as the indices  $i$ ,  $k$ , and  $l$  would simply have more values. If the original model were not a quasi-nondivergent model but a "primitive" equation model, the right-hand side of the energy equations would be different; however, the energy diagram in figure 5 would still be the same.

The advantage of the stochastic dynamic method and of these energy equations is that one can *quantify* the growth of uncertainty. Various calculations are included in this paper to bring this point out. Here, however, we will only qualify certain features of the energy diagram shown in figure 5.

Numerical computations indicate that the largest energy conversion (involving an uncertain energy) is  $A_Z$  to  $UA_E$ . This is associated with baroclinic instability as is the conversion  $A_Z$  to  $A_E$ . Large-scale baroclinic instability is the prime mechanism for transporting heat from low latitudes to higher latitudes. The resulting large-scale eddies are of importance in maintaining the general circulation of the earth's atmosphere against frictional dissipation. It is not surprising that if the physical variables involved in such a large-scale nonlinear mechanism are not perfectly known initially, the future values of those variables (after the instability mechanism has had time to work) will be known even less perfectly. This situation reaches the worst possible stage when the "true" values of the variables are near a critical condition where instantaneous development may or may not occur.

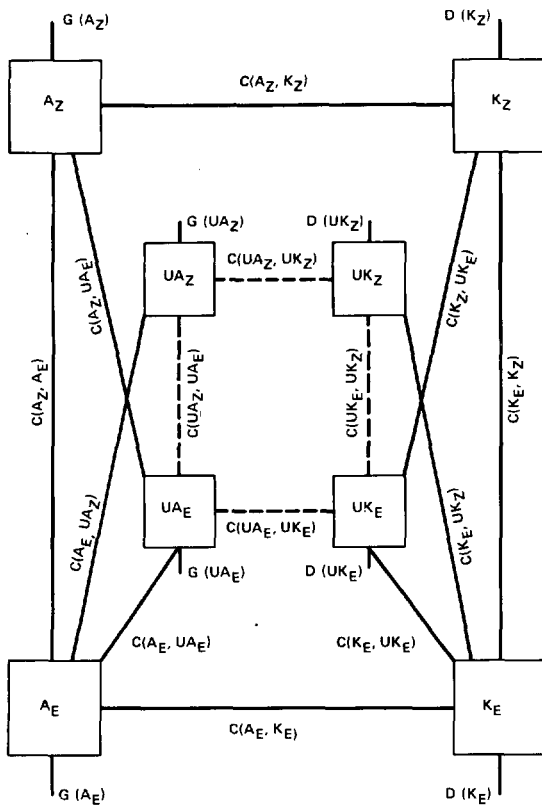


FIGURE 5.—Stochastic dynamic energy diagram.

The conversions  $C(A_Z, UA_E)$  and  $C(A_E, UA_Z)$  given by eq (56) and (57) show the extent of this nonlinear growth of uncertainty. Both conversions are concerned with the uncertain transport of an uncertain amount of heat northward, but the former is by far the most important as it involves the certain or mean latitudinal temperature gradient (a relatively large quantity) multiplying uncertain eddy components, while the latter conversion involves certain eddy temperatures (relatively small quantities) multiplying terms involving the uncertainty of latitudinal temperature gradient (and other terms) which tend to remain small, relatively speaking.

The conversions  $C(K_E, UK_Z)$  and  $C(K_Z, UK_E)$  involve barotropic instability. These conversions are much smaller than  $C(A_Z, UA_E)$ , as would be expected since barotropic instability plays the lesser role in the real atmosphere. These conversions are discussed in this section.

The conversions  $C(A_E, UA_E)$  and  $C(K_E, UK_E)$  are due to the nonlinear exchange of energy between wave numbers other than zero, that is, the eddies. These conversions can and do change sign, but their amplitudes are small and they will not be referred to in the remainder of this paper.

The conversions  $C(UA_Z, UK_Z)$  and  $C(UA_E, UK_E)$  involve the variance of the vertical velocity, which is reasonable, since the conversions  $C(A_Z, K_Z)$  and  $C(A_E, K_E)$  involve the vertical velocity in the deterministic calculation, and involve the expected value of the vertical velocity in this stochastic calculation. There are, however, missing terms in eq (54) and (55) for the uncertain conversions. The

reason is simply that the vertical velocity involves a Jacobian, which in turn implies that eq (54) and (55) involve a triple correlation of moments about the mean. Up to this point, we have used the simple closure scheme of neglecting third moments. It is, therefore, necessary to keep third moments if an accurate account of  $C(UA_Z, UK_Z)$  and  $C(UA_E, UK_E)$  is to be made. These additional terms are described later in this paper when the problem of closure is discussed.

Up to this point, the uncertain generations and dissipations are necessarily constrained to act in such a way as to remove uncertainty; that is,  $G(UA_Z)$  and  $G(UA_E)$  will be negative (removing energy from their respective boxes) and  $D(UK_Z)$  and  $D(UK_E)$  will be positive (removing energy from their respective boxes). This occurs because the physical parameters we have used to simulate the forces working on the atmosphere have been assumed to be known perfectly. This is what all deterministic forecast and simulation models do, also. The implications of this assumption are discussed in part II, but the effects on the energy generation are discussed in a later section of this paper.

Figure 5 reveals no conversion from  $A_Z$  to  $UA_Z$  and  $K_Z$  to  $UK_Z$ . This is because there is no communication between the means of the zonal quantities and their respective variances. This, in turn, is because the deterministic prognostic equations for the zonal components do not contain other zonal components in the nonlinear terms on the right hand side of their respective expressions.

#### ENERGY FLOW IN A BAROTROPIC SYSTEM

The energy flow characterized by figure 5 will be shown in numerical calculations. Fortunately, there are physical situations in which the numerical calculations must give *exactly* predictable results—this will suggest that the computer program is working properly. Numerical calculations of the *complete* energy conversions using eq (40) through (61) were carried out to convince the author that those *conversion* equations were correct. By adding from the conversions the input and output to each energy "box" (through a complete Kutta-Simpson time step), we should obtain net changes that exactly agree with the energy box values before and after the time steps. Such calculations were instrumental in discovering initial algebra errors, but eventually these calculations were "exact", well within the bounds of roundoff error.

The simplest case to consider is reversion back to a barotropic model by assuming that all  $\theta_i$ , linear terms, and constant terms are equal to zero. In this model, the sum of zonal and eddy kinetic energy is conserved. The energy diagram reduces to that of figure 6.

The total energy in the four boxes must be constant for all time. Results for a particular case are shown in table 1. It is seen that the required energy is conserved. The last digit in the total is in doubt because of the printing format used, but there is an extremely small "time" truncation error as well as roundoff error present. Waves 2, 4, and 6 were used in this case. The time step was equivalent to 1.5 hr.

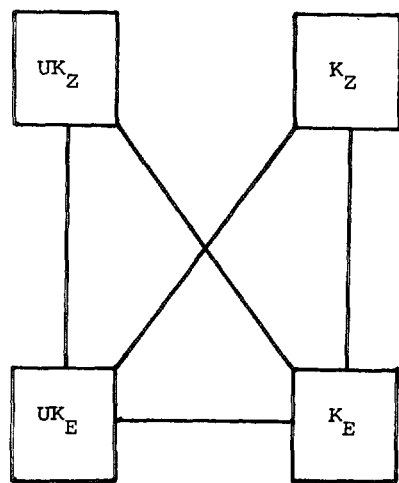


FIGURE 6.—Barotropic stochastic dynamic energy diagram.

TABLE 1.—Barotropic energy conservation ( $\text{kJ} \cdot \text{m}^{-2}$ )

Time (days)	$K_Z$	$K_E$	$UK_Z$	$UK_E$	Total
0	1040.0	1120.0	10.0	172.0	2342.00000
7	728.1	832.0	269.5	512.4	2342.00001
14	766.7	403.6	167.8	1003.9	2342.00004
21	821.8	470.8	220.3	829.1	2341.99997

An important point concerning the value of the stochastic dynamic equations is brought out in table 1. There is not much that can be said about the eddies after two weeks, as  $UK_E$  is about two and one-half times as great as  $K_E$ . Note that at 3-weeks, however, there is more certain energy in the system. The stochastic dynamic model does not allow the uncertainty to grow without limit—and this is realistic. In a barotropic flow, the energy distribution oscillates back and forth with more energy alternately in the zonal component and eddy component. A characteristic period of 5 to 6 days for this process is shown by Thompson (1957), Wiin-Nielsen (1961), and others. At 2 weeks, a greater portion of the energy is in the eddies but there is great uncertainty as to exactly where the eddies are! The dynamics of the model then dictate that the eddies should feed back their energy to the zonal flow, and at 3 weeks this has happened. The uncertain eddies give up their energy properly because the stochastic dynamic equations keep track of the uncertainties “dynamically.” The flow is actually more predictable at 3 weeks than at 2 weeks. The zonal component is more predictable than any eddy components; there is one less degree of freedom.

The growth of uncertainty in a barotropic model is studied with two cases having the same initial energy. The two cases differ only in the specification of the mode “2” zonal component amplitude,  $\psi_2$ , which results in an initially stable or unstable barotropic flow. Only the sign of this component is changed so that the energy is the same in each case; however, the sign change results in satisfying instability requirements.

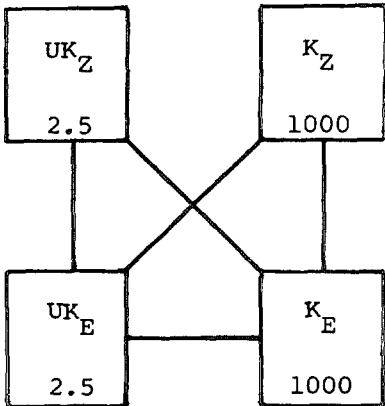


FIGURE 7.—Initial energy conditions for stable-unstable barotropic test. Energy is in  $\text{kJ} \cdot \text{m}^{-2}$ .

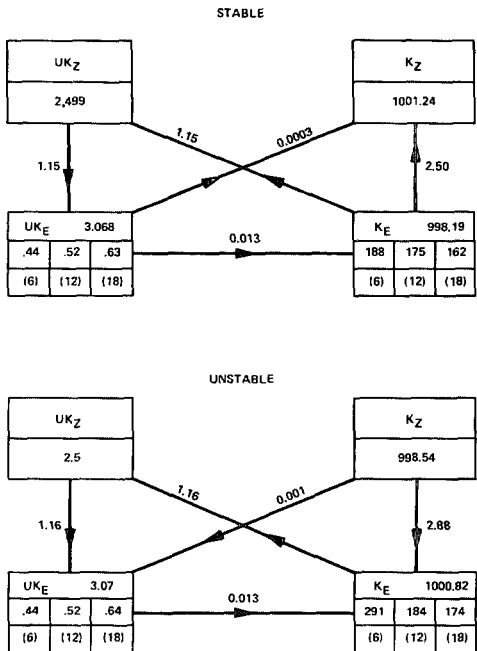


FIGURE 8.—Energy conditions after 3 hr for stable-unstable case with  $E$  in  $\text{kJ} \cdot \text{m}^{-2}$ ,  $\dot{E}$  in  $10^{-4} \text{kJ} \cdot \text{m}^{-2} \cdot \text{s}^{-1}$ .

Figure 7 shows the initial conditions of each case where appropriate values of  $\psi_i$  have been chosen to give the indicated energies. Waves 6, 12, and 18 in the  $x$ -direction are chosen. Figure 8 shows the energy values and conversion rates after 3 hr. In the stable case, the waves are feeding energy to the zonal flow, while the reverse is true for the unstable case, where the waves are growing at the expense of the zonal flow. Note that in both cases the growth of uncertainty is through  $C(K_E, UK_Z)$  and subsequently  $C(UK_Z, UK_E)$ . The uncertain energy  $UK_Z$  is acting as a “catalyst” in the early stages of this growth of uncertainty.

A look at the behavior of the kinetic energy in mode “1” of waves 6, 12, and 18 is also given in figure 8. Initially, each wave had the same amount of certain and uncertain energy. Since wave 18 is more stable than the other waves,

TABLE 2.—Energy check for adiabatic frictionless model with energy in the units  $\text{kJ} \cdot \text{m}^{-2}$ 

Weeks	$A_z$	$A_E$	$K_z$	$K_E$	$UA_z$	$UA_E$	$UK_z$	$UK_E$	Total
0	10,000	3926	1200	1200	100	39	12	12	16,489.300
1	1,628	2680	634	1886	400	5497	78	3685	16,487.881
2	277	1402	480	1055	1225	7139	380	4527	16,487.791
3	424	3276	1948	444	1683	342	6172	181	16,487.569
4	114	2254	435	1435	832	5954	472	4990	16,487.411
5	142	1195	416	8803	1665	6738	468	5059	16,487.275
6	21	1604	421	963	1027	6852	276	5321	16,487.069

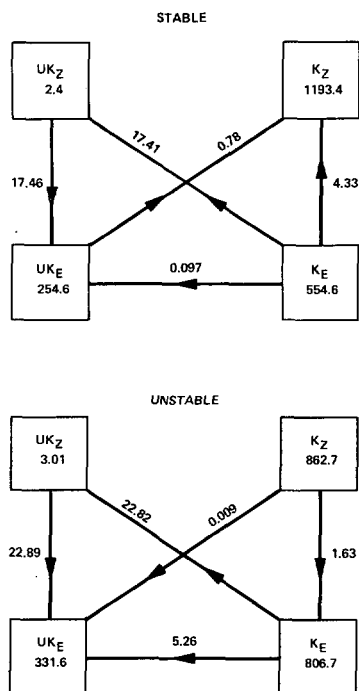


FIGURE 9.—Energy conditions after 3 days for stable-unstable case. Units are the same as in figure 8.

it gives up its energy faster in the stable case. Wave 6 is more unstable than the other waves and is gaining energy faster in the unstable case. However, in both cases, the growth of uncertainty is greater in the smaller scales or higher wave numbers. If the energy diagram were further broken down to show relations within wave numbers, the cascade of uncertain energy to the higher wave numbers would be seen. That the smaller-scale errors should grow faster is nothing new or unnatural. Consider just a linear displacement of a small-scale feature by the zonal wind or by a large-scale wave. A small uncertainty in the large scale has a large effect on the small scale, as discussed by Lorenz (1969).

Figure 9 shows the energy and energy transforms at 3 days. The stable case has less total uncertainty. Thus, 3-day forecasts from initially stable situations will have better verification scores, or, in other words, the forecasts can be made with greater confidence. The stochastic dynamic method gives the expected state and a measure of that confidence.

### ENERGY FLOW IN AN ADIABATIC FRICTIONLESS SYSTEM

A more complex model, with more degrees of freedom than the barotropic, results if the  $\theta_i$  are retained. The linear and constant terms are still zero. This is the adiabatic frictionless model. Figure 5 gives the corresponding energy diagram (with the removal of the generations and dissipations) and the sum of the energy of the boxes is constant with time. Numerical results for a typical case (table 2) show that this energy is conserved even when the integration in time is carried far past the unpredictable stage. This model is the least predictable, as is discussed in part II; its value here lies in the check it provides on the energy equations and the model itself. The integration has been carried out to 6 weeks with waves 2, 4, and 6 and a time step of 3 hr.

### CERTAIN-UNCERTAIN ENERGY FLOW IN A BAROCLINIC SYSTEM

The values of the heating and friction coefficients as well as the choice of  $\sigma$  will determine the type of motion that will evolve. In a classic study showing the power of this simple two-level spectral model with but a single wave in the  $x$ -direction, Lorenz (1963b) was able to reproduce the different regimes of flow found in the rotating-annulus experiments of Hide (1953), including an irregular non-periodic flow typical of the atmosphere. In that study, Lorenz let  $h=\kappa=2\kappa'$  so that the controllable external parameters were  $\theta_1^*$  and  $h$ . Starting with a weak zonal flow with small superimposed perturbations, the different regimes of flow occurred for different external parameters.

For his predictability experiment, Lorenz (1965) used three waves in the  $x$ -direction, and values of  $\sigma$ ,  $\theta_1^*$  and  $h$  were chosen to give irregular nonperiodic flow. This study follows Lorenz in setting  $h=\kappa=2\kappa'$ . The purpose of this paper is to study stochastic concepts and not to simulate the atmosphere (which could hardly be accomplished by a two-level model). Nevertheless, it is desirable to choose parameters that give irregular nonperiodic flow resembling the flow patterns found in the atmosphere. This has been achieved by using values  $\theta_1^*=9/128$ ,  $h=15/128$ , and  $\sigma=5/128$ . The values of  $\theta_1^*$  and  $h$  are slightly less than those used by Lorenz (1965) for reasons given in part II. Only  $\theta_1^*$  was retained in the linear term, implying a heating at the Equator and a cooling at the poles. Changes of these parameters are used in this study to

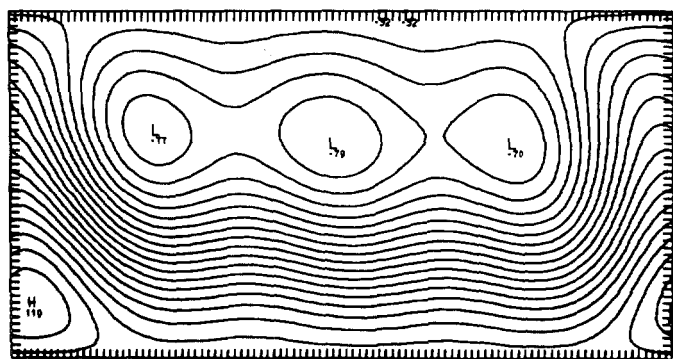


FIGURE 10.—Initial stream field  $\psi$  of "return to Hadley circulation" case.

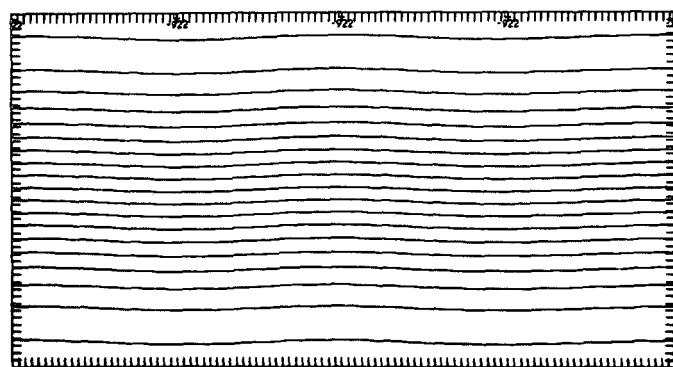


FIGURE 11.—Stream field after 3 weeks of return to Hadley circulation case.

clarify various concepts. When such changes are made, the new values are given.

Energy is no longer conserved in the model when forcing and friction are included. However, an additional check is devised to insure that the stochastic dynamic energy equations are correctly derived and correctly programmed. A large value of  $\sigma$  is used in a complex initial state of large eddies. The large  $\sigma$  means that the upper level has a much higher potential temperature than the lower layer—a very stable situation. With this stable atmosphere containing frictional dissipation, the flow in the model should return to the steady-state Hadley circulation which has an analytical solution discussed by Lorenz (1963b).

For this run only, the value of  $\sigma$  is double its commonly used value, that is,  $\sigma = 10/128$ . The initial stream field for this case is shown in figure 10. The resulting flow after 3 weeks is shown in figure 11. The flow is approaching the equilibrium Hadley circulation with the proper analytical values for  $\psi_1$  and  $\theta_1$ . These values are obtained by solving eq (9) and (10) for the steady-state zonal flow which yields:

$$\theta_1 = \psi_1 \quad (62)$$

and

$$\theta_1 = \theta_1^*/(1 + \sigma) \quad (63)$$

The initial values of  $\psi_1$  and  $\theta_1$  were 0.0452 and 0.0442,

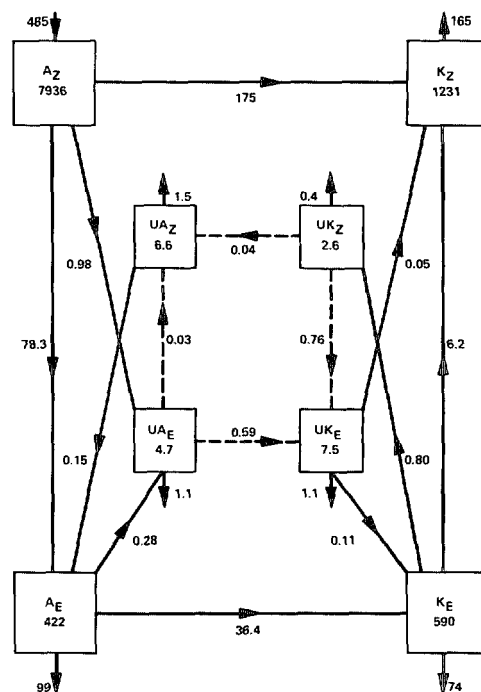


FIGURE 12.—Energy after 1 day for return to Hadley circulation case with  $E$  in  $\text{kJ} \cdot \text{m}^{-2}$ ,  $\dot{E}$  in  $10^{-4} \text{ kJ} \cdot \text{m}^{-2} \cdot \text{s}^{-1}$ .

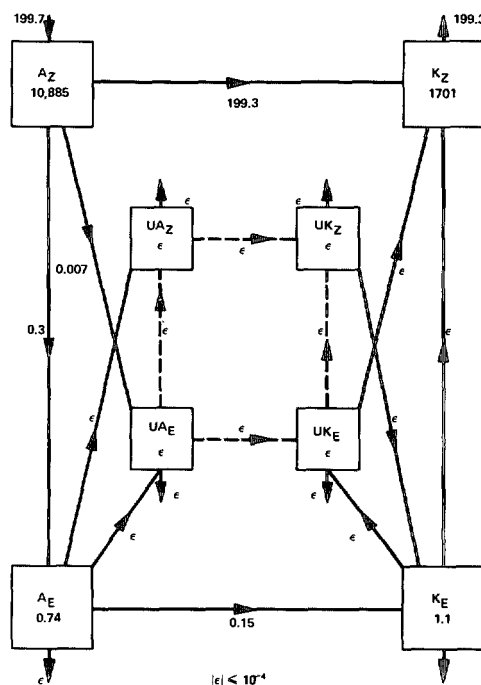


FIGURE 13.—Energy after 3 weeks for return to Hadley circulation case. Units are the same as in figure 12.

respectively—they converged to the common value of 0.06521 which satisfies eq (63). The energy diagrams in figures 12 and 13 show that the stochastic dynamic energy equations are programmed correctly. The eddy energy and exchanges have nearly vanished, and the terms  $G(A_Z)$ ,  $C(A_Z, K_Z)$ , and  $D(K_Z)$  are approaching a steady-state common value.

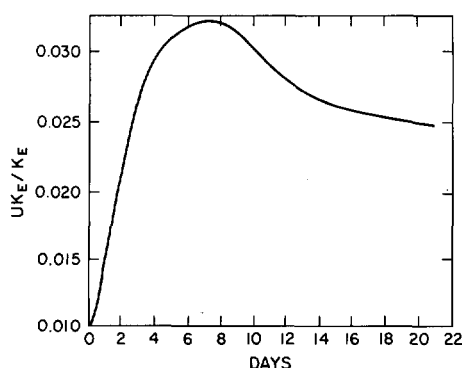


FIGURE 14.—Relative kinetic energy uncertainty as a function of time in the return to Hadley circulation case.

Another important point is brought out by this case. The relative error of the eddies ( $UK_E/K_E$ ) is decreasing. It is natural to expect that the absolute uncertainty of the eddies will drop because of the dissipation of the eddies themselves, but it is not obvious that the relative uncertainty would drop. In the barotropic case, it was seen that when the situation was stable, the relative uncertainty was greater than in the unstable case. Figure 14 shows the relative uncertainty as a function of time. The stochastic equations are energetically consistent and keep track of the uncertainty dynamically. As a result, the volume of the ensemble of points in phase space will eventually shrink to a single point—the same point that the deterministic trajectory will ultimately arrive at—the steady-state solution of the phase variables.

A particular example of the resulting energy transformation for the barotropic case with irregular flow is considered next. Many different calculations were made by varying different initial conditions and forcing parameters. Quantitative discussions of these values and how they change will not be a part of this paper. Moreover, such a discussion may be of little value in that this baroclinic model is so severely truncated and contains the physically inhibiting use of a constant static stability (cf. Lorenz 1960). However, the *qualitative* effect of the growth of uncertainty can be assessed; in particular, the *relative* values of different uncertain energy conversions are typified by the example shown in figures 15 and 16.

Figure 15 (left) shows an initial state of a particular case and the resulting energy values and conversions after 1 day (right). Figure 16 shows these values after 1 and 2 weeks. Choosing and maintaining energy values corresponding to atmospheric values is somewhat difficult (and perhaps meaningless) with such a severely truncated system. However, the initial energy values are close to winter values (cf. Wiin-Nielsen 1967) except for  $A_Z$  which is too large by a factor of two. The latter was necessary to maintain nonperiodic flow in such a truncated system and this will be further discussed in part II.

Three general comments typical of all calculations and indicated in figures 15 and 16 are: (1) the conversion  $A_Z$  to  $UA_E$  dominates in the growth of uncertainty; (2)

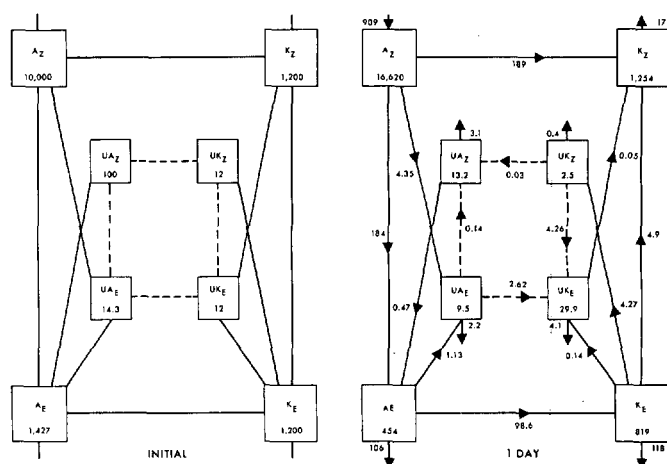


FIGURE 15.—Energy conditions in a case of irregular baroclinic flow initially and after 1 day with  $E$  in  $\text{kJ} \cdot \text{m}^{-2}$ ,  $\dot{E}$  in  $10^{-4} \text{kJ} \cdot \text{m}^{-2} \cdot \text{s}^{-1}$ .

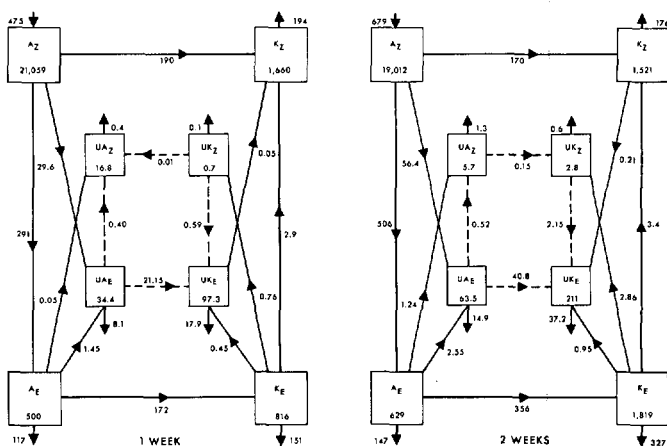


FIGURE 16.—Energy conditions in a case of irregular baroclinic flow after 1 week and after 2 weeks. Units are the same as in figure 15.

the resulting uncertain energy values are considerably smaller for zonal components than they are for eddy components; and (3) the effects of heating and friction tend to slow the growth of uncertainty by acting to reduce the variances of the variables; that is, there is negative generation and positive dissipation of what has been called the uncertain energy. This is considered in greater detail in the following section.

## 6. EFFECTS OF IMPERFECT FORCING ON ENERGETICS

The atmosphere is *primarily* forced by net radiative heating at the Equator and cooling at the poles. However, there are *secondary* forces present which will vary with latitude and longitude, including complex radiation processes; release of latent heat and evaporation in precipitation processes; conduction of sensible heat; etc. None of these atmospheric processes is known perfectly, although some are known considerably better than others. A



prediction model simulates these processes by various parameters. The question that must be answered is, "How does uncertainty in the physical parameters affect predictability?" The stochastic dynamic equations can provide answers to this question, but to understand these answers the energetics will be utilized.

Consider, for example, that the  $\theta_i^*$  are still constant but that their values are uncertain. There is then a mean and variance for each  $\theta_i^*$  that contributes to the forcing. Thus, their deterministic tendencies are zero (being in the general form of eq (2) with the  $a$ 's,  $b$ 's, and  $c$ 's all zero) and the stochastic dynamic equations involving the  $\theta_i^*$  only become

$$(\dot{\theta}_i^*)=0 \quad (64)$$

and

$$[\text{cov}(\dot{\theta}_i^*, \dot{\theta}_j^*)]=0. \quad (65)$$

Thus, the means and covariances involving only the  $\theta_i^*$  do not change. However, even though  $\text{cov}(\theta_i, \theta_i^*)$  may be initially zero, it is readily shown (cf. Fleming 1970) that correlations between the  $\theta_i$  and  $\theta_i^*$  will develop.

The effect of the terms  $\text{cov}(\theta_i, \theta_i^*)$  on the energetics is considered in the following where *previous* energy terms are assumed present. Then eq (22) becomes

$$[\text{var}(\dot{\theta}_i)] = \dots + \frac{2h}{\sigma a_i^2 + 1} \text{cov}(\theta_i, \theta_i^*) = \dots + 2FU \quad (66)$$

where

$$FU = \frac{h}{\sigma a_i^2 + 1} \text{cov}(\theta_i, \theta_i^*) \quad (67)$$

Then eq (29) becomes

$$\dot{A} = \dots + [\dots - a_i^2 FU] + \left( \frac{a_i^2 \sigma + 1}{\sigma} \right) FU \quad (68)$$

Carrying this term through the ( $\dot{K}$ ) equation reveals that  $-a_i^2 FU$  completes the definition of the uncertain vertical velocity. The term  $[(a_i^2 \sigma + 1)/\sigma] FU$  is seen to be another component of the generation of uncertain available potential energy. When these are added to their respective energy equations they become

$$C(UA, UK) = \dots + \left( \frac{a_i^2}{\sigma a_i^2 + 1} \right) h \text{cov}(\theta_i, \theta_i^*) \quad (69)$$

and

$$G(UA) = \dots + \frac{h}{\sigma} \text{cov}(\theta_i, \theta_i^*). \quad (70)$$

Thus, the inclusion of the notion of uncertainty in the diabatic heating contributes directly to the generation of uncertain available potential energy and to the conversion of  $UA$  to  $UK$ . Indirectly, it eventually contributes to all the terms.

The difference in expressing the physical forcing "perfectly" versus expressing it "imperfectly" is fully

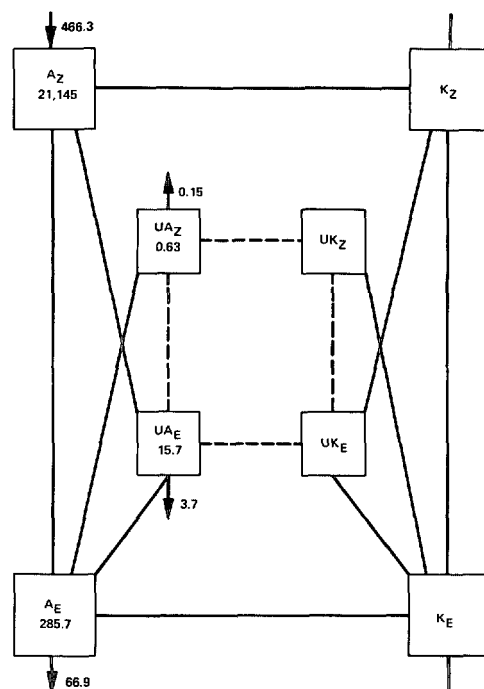


FIGURE 17.—Partial energy diagram after 3 days for a typical case where primary forcing is known "perfectly." Units are the same as in figure 15.

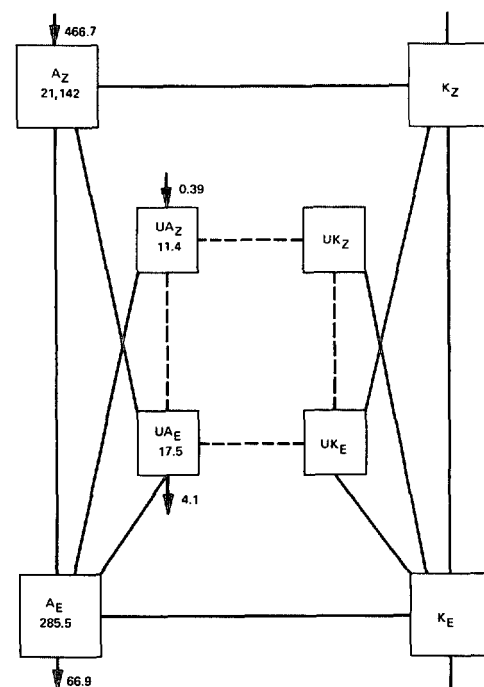


FIGURE 18.—Partial energy diagram after 3 days for same case as figure 17, but primary forcing parameter has 2.5 percent standard deviation. Units are the same as in figure 15.

brought out in part II. A manifestation of that difference is revealed in figures 17 and 18 where partial energy diagrams are shown for two different cases dealing with primary forcing. In one case, the primary forcing is

assumed to be known perfectly; in the other case, the  $\theta_i^*$  has a standard deviation of 2 1/2 percent of the mean value of  $\theta_i^*$ . (The details of the initial conditions are not given here, as any set of conditions will show the qualitative result that is brought out.)

Note that in the "perfect" forcing the  $G(UA_z)$  is negative, and when the forcing is "imperfect" the generation of the zonal component of uncertain available potential energy is positive. From eq (48), with no uncertainty in the heating term,  $G(UA_z)$  is necessarily negative. The heating in the model is such that the largest latitudinal temperature gradients are reduced and vice versa. Diabatic heating tends to eliminate uncertainty and push the system toward equilibrium. But if the heating is uncertain, temperatures would get higher if heating is large and vice versa,  $\theta_i$  and  $\theta_i^*$  will become positively correlated, and  $G(UA_z)$  may (and does) become positive [cf. eq (70)].

Many interesting calculations that highlight the growth of error can be made with the energy equations. The nature of this paper will only permit a summary here.

We have stated that, by dealing with the uncertainty dynamically, the expected forecast of an uncertain ensemble of initial conditions can result and the growth of uncertainty of the forecast can be viewed through the energetics. It has been shown that the stochastic dynamic equations that neglect third and higher order moments conserve the ensemble energy in those cases where the energy should be deterministically conserved. Epstein (1969b) has pointed out that, while dropping the third moments implies that the time derivatives of the individual variances are inexact, the equation for the time derivative of his kinetic energy did not contain third moments. This is indeed true and is the reason that the sum of the energy in the eight boxes of an adiabatic frictionless energy diagram is conserved. It is not assured that the energy *exchange* between these boxes is "accurate." This last point is emphasized in the following section.

## 7. THE CLOSURE PROBLEM

Epstein (1969b) has made the solution of the stochastic dynamic equations tractable by simply disregarding third and higher order moments. He notes that this closure scheme is necessary in light of the vast amount of computation required. He also notes that the success of the deterministic equations, which are but a form of the general stochastic dynamic equations with the variances implicitly assumed to be zero, suggests that the truncated set will be more successful than the deterministic, and should be valid if the time domain is not too large. However, there is evidence that this closure is not a good one. That third moments which are initially small or zero will not significantly alter the forecast of the first moments until they become large is not an obvious fact. It is possible that the sum effect of *many* small third moments will be significant. There is also the question of their

effect on the second moments. To underscore this last concern, consider the history of analytical theories of turbulence.

The present day analytical theories of turbulence originated from the statistical approach of Taylor (1921). These theoretical investigations are usually limited to the idealistic case of homogeneous isotropic turbulence. Homogeneity means that the statistical properties of the space domain of turbulence are independent of position in that domain, and isotropy means that the properties are independent of direction. The method of obtaining the statistical moments of the velocity field from the Navier-Stokes equation leads to the same type of closure problem faced in stochastic dynamic prediction of the primitive equations. The assumption of homogeneity, however, leads to a tremendous simplification of the equations, that is, the mean velocity can be considered zero. After obtaining the Fourier transformation of the Navier-Stokes equation, the variance of the Fourier components of the velocity field is then proportional to the turbulent energy, and the third moments are necessary for nonlinear transfer of energy between eddies. A closure technique that was considered for many years was the quasi-normal theory of Millionshtchikov (1941) and Proudman and Reid (1954). This scheme retains a prognostic equation for the third moments but relates fourth moments to second moments by assuming a Gaussian distribution. It was pointed out by Ogura (1963) that negative values of energy are obtained from this closure scheme after a finite length of time. The effect of dropping third moments is not as drastic as in homogeneous turbulence, but its effect must be investigated.

## RELATION OF CLOSURE TO ENERGETICS

Insight into the effect of the third moments is gained from considering their effect on the energetics. The effect is only derived for the kinetic energy equation in a barotropic model, but the results for a baroclinic model can similarly be evaluated and are only stated below. Considering only the third moment term, one can write

$$[\text{var}(\psi_i)] = \dots + 2 \sum_{k,l} a_i^{-2} (a_k^2 - a_l^2) C_{ikl} \tau_{ikl}. \quad (71)$$

Again, considering only this term, one obtains

$$\dot{K} = \dots + (a_k^2 - a_l^2) C_{ikl} \tau_{ikl} \quad (72)$$

where the right-hand side would fall under the notation  $AMU$  as defined in the original energy equation development of the previous section. With the technique used in discussing term "9" in eq (29), it is readily seen that the third moment adds to the definition of  $C(UK_E, UK_Z)$ . If the variables  $\theta_i$  were included, the third moments in the temperature equation would become part of the term labeled  $ASU$  and would be seen to contribute to  $C(UA$ ,

UK) and  $C(UA_Z, UA_E)$ . Consideration of each distinct triplet also reveals that nonlinear exchange of uncertain energy between wave numbers is now possible where it was not possible when the third moments were dropped. In the turbulence theory, this latter energy transfer is the nonlinear turbulent energy transfer between eddies.

The important point here is that even though Epstein's simple closure scheme assures conservation of total energy (certain and uncertain) in those physical systems where it should be conserved, the neglect of the third moments yields the result that the correct allocation of energy to specific "boxes" is not assured. The consequences of that misappropriation must be investigated.

One may summarize the effects of the third moments by noting that they do not affect the conservation of energy. They are not explicitly involved with any conversion of certain to uncertain energy, but they are explicitly involved in all transfers between uncertain energy components. Of course, if a nonlinear transfer between uncertain modes is incorrect, the subsequent exchange between those modes and certain modes will be affected. Evidently, one must consider numerical calculations which contain third moments to judge their effect on the other statistical properties.

#### QUASI-NORMAL CLOSURE AND CONGRUENCY

The derivation of a prognostic equation for third moments proceeds in the same manner as that used in deriving such an equation for the second moments (cf. Fleming 1970). Following the general form for the primitive equations given in eq (2), the prognostic equation for the third moments is given by

$$\begin{aligned} \dot{\tau}_{jkl} = \sum_{p,q} \left[ a_{jpq}(\mu_p \tau_{k l q} + \mu_q \tau_{k l p} - \sigma_{pq} \sigma_{kl} + \lambda_{k l p q}) \right. \\ \left. + a_{kpq}(\mu_p \tau_{j l q} + \mu_q \tau_{j l p} - \sigma_{pq} \sigma_{jl} + \lambda_{j l p q}) \right. \\ \left. + a_{lpq}(\mu_p \tau_{j k q} + \mu_q \tau_{j k p} - \sigma_{pq} \sigma_{jk} + \lambda_{j k p q}) \right] \\ - \sum_p (b_{jp} \tau_{k l p} + b_{kp} \tau_{j l p} + b_{lp} \tau_{j k p}) \quad (73) \end{aligned}$$

where  $\lambda$  refers to fourth moment about the instantaneous mean. One must now make assumptions about the fourth moments or derive an equation for them and make assumptions about the fifth moments. The closure scheme considered here is analogous to the quasi-normal theory used in turbulence theory. Assuming that the initial values are multivariate normally distributed, an expression for the general fourth moment about the mean,  $\lambda_{k l p q}$ , can be found by generating the first, second, third, and fourth moments from the moment generating function. The fourth moment about the mean can then be expressed as

$$\lambda_{k l p q} = \sigma_{kl} \sigma_{pq} + \sigma_{kp} \sigma_{lq} + \sigma_{kq} \sigma_{lp}. \quad (74)$$

In a multivariate normal distribution, the third moments are identically zero and the fourth moments are

expressible as products of second moments. If this expression is used in eq (73), the system of equations is closed, but since it is used in the third moment equation, one can see how the "quasi" term originates. Inserting eq (74) into (73) yields

$$\begin{aligned} \dot{\tau}_{jkl} = \sum_{p,q} \left[ a_{jpq}(\mu_p \tau_{k l q} + \mu_q \tau_{k l p} + \sigma_{kp} \sigma_{lq} + \sigma_{kq} \sigma_{lp}) \right. \\ \left. + a_{kpq}(\mu_p \tau_{j l q} + \mu_q \tau_{j l p} + \sigma_{jp} \sigma_{lq} + \sigma_{jq} \sigma_{lp}) \right. \\ \left. + a_{lpq}(\mu_p \tau_{j k q} + \mu_q \tau_{j k p} + \sigma_{jp} \sigma_{kq} + \sigma_{jq} \sigma_{kp}) \right] \\ - \sum_p (b_{jp} \tau_{k l p} + b_{kp} \tau_{j l p} + b_{lp} \tau_{j k p}). \quad (75) \end{aligned}$$

Before evaluating this closure scheme we ask, "How can the merit of any closure scheme be verified?" We are concerned with more than just the verification of the original  $N$  dependent variables. We are interested in the evolution of the joint probability distribution of all those variables; less demanding, we wish to know if the dynamic coupling between those variables and the measure of uncertainty associated with them is "representative" based upon all the associated uncertainties which have been discussed. Since arriving at the true distribution requires solving the infinite set of moment equations, we settle for an approximation of the distribution. This is achieved by considering a great many samples in a Monte Carlo calculation as used by Epstein (1969b).

In the Monte Carlo method used here, a sample is selected from the ensemble of points in phase space. The points are obtained at random from a multivariate normal distribution with a preassigned mean and variance for each variable corresponding to the same mean and variance used in a stochastic dynamic method. The deterministic trajectories in phase space are then determined for each of the points. The results of each of the deterministic forecasts are accumulated in an array at specific times and any desired statistical quantity such as the mean, variance, etc., is computed from that array. When a great many deterministic trajectories are computed out to time  $t_1$  the mean of those values at time  $t_1$  is a good estimate of the expected value. Thus, the collective behavior of a great many samples in a Monte Carlo method gives the "norm" by which a closure scheme can be measured.

Obtaining a good approximation to higher order moments may demand an extremely large sample size; that size will be further compounded by the inclusion of uncertain forcing parameters. Nevertheless, we shall define "congruency" in an order of moments to mean that they are "superposable so as to coincide throughout" with Monte Carlo moments of the same order. Ideally, all the moments of a closure scheme should be congruent with their Monte Carlo counterparts. As the forecast period is extended, however, the effect of dropping the higher order moments will eventually destroy that congruency—even

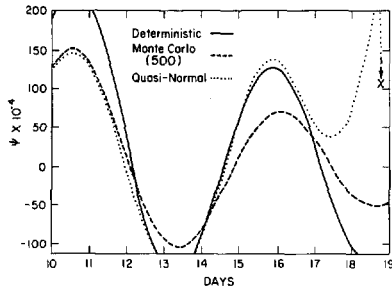


FIGURE 19.—Comparison of quasi-normal closure by showing cosine components of wave 4.

down to the lowest order moment, the mean. Congruency, at least in the lowest order, must be maintained in a stochastic dynamic forecast. It makes little difference how large the uncertainty becomes because each forecast user must determine his own limit of uncertainty. There is much useful information in knowing how uncertain a forecast is—plans can be formed from this information—but the integrity of the mean must be maintained or that information may be useless.

The stochastic dynamic calculations that include third moments must be restricted to a barotropic model because of the vast amount of storage required. Such a calculation is shown in figure 19. The  $\psi_i$  had values ranging from 0.00 to 0.06. The initial variance of each  $\psi_i$  was  $1.0 \times 10^{-5}$ . Waves 2, 4, and 6 were considered in this case, and the value of the cosine component of wave 4 is plotted as it evolved in three types of forecasts: the deterministic, the stochastic dynamic with quasi-normal closure, and the Monte Carlo.

It is seen that at 10 days, the quasi-normal closure scheme is still congruent in the mean, being very close to the Monte Carlo; and that both differ from the deterministic solution. After 11½ days, the first negative variance appeared in the quasi-normal calculation. At 18¼ days the calculation begins to “blowup”. The reason for the blowup is not the negative variance itself, but rather that energy is flowing from the uncertain boxes to the certain boxes at an ever-increasing rate. The sum of the energy is still conserved, but only because the uncertain energy is becoming more and more negative with the certain energy becoming more and more positive, eventually resulting in an overly strong zonal flow that violates linear computational stability. The initial kinetic energy (certain and uncertain) was 2,342 units and the maximum zonal wind in the southern part of the channel was 34 m/s. After 19 days, the total kinetic energy was still remarkably conserved, being 2,340.4 units. However,  $UK_E$  was -20,261 units with the large positive balance spread over  $K_Z$ ,  $K_E$ ,  $UK_Z$ , and the zonal wind in the southern part of the channel had reached 91 m/s.

Orszag (1970) shows that the failure of the quasi-normal closure in homogeneous isotropic turbulence calculations can be attributed to the theory's lack of a dynamically-

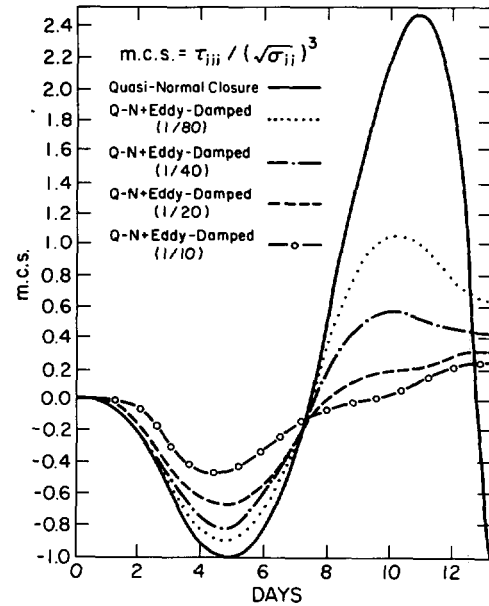


FIGURE 20.—Plot of moment coefficient of skewness of  $\psi_8$ .

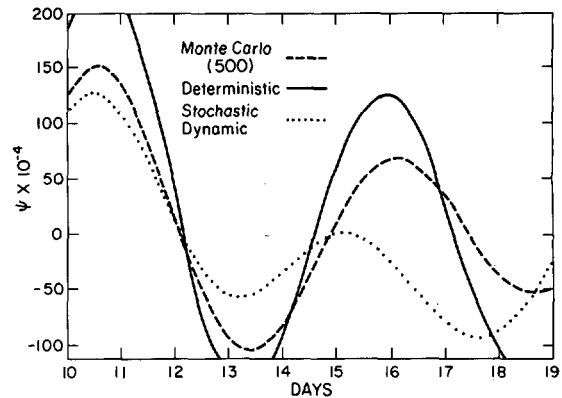


FIGURE 21.—Comparison of stochastic dynamic closure with no third moments by showing cosine components of wave 4.

determined relaxation time—so that no slightly perturbed steady state can be approached. He shows numerical calculations of a weakly driven model system that begins with an initial equilibrium ensemble which should relax to a new stationary state. However, the system overshoots its new stationary state, and the energy density of some of the wave numbers is seen to oscillate with increasing amplitude as time increases. A very similar effect is seen in figure 20 where the “moment coefficient of skewness” (m.c.s.) of one of the components is shown. This computation is based upon the results of the same case shown in figure 19. One sees that the moment coefficient of skewness increases without bound.

The results of the simpler scheme of dropping third moments for the same case are shown in figure 21. The figure shows that this scheme is realizable; in fact, other cases showed no tendency for negative energy out to 6 weeks. But this simple closure scheme does not maintain congruency for as long as might be desired. Deviations

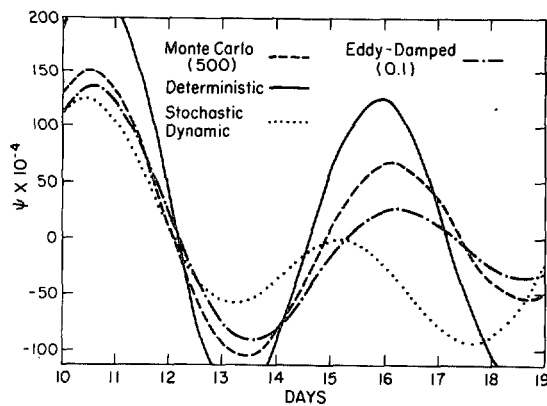


FIGURE 22.—Comparison of eddy-damped closure by showing cosine components of wave 4.

from the Monte Carlo solution become important after 13 days.

#### EDDY-DAMPED CLOSURE

In dealing with analytical theories of homogeneous isotropic turbulence, a number of authors have tried to incorporate a damping effect on the third moments while retaining the quasi-normal assumption. Early work in this area was done by Edwards (1964) and more recently by Orszag (1970) and Leith (1971). The growth of the third moments is thus stymied by a damping term that is intended to simulate the "natural" damping of triple correlations that would take place if all the higher ordered moments were included. What this damping factor should be, or what it should be a function of, has not been analytically determined.

It will be important to know if the simplest type of damping will work in the stochastic calculations, because if so, then a more complicated form may ultimately be available. With this motivation, consider the eddy-damped form of the quasi-normal forecast equation of the third moments, eq (75), to be

$$\dot{\tau}_{jkl} = \dots + [\text{quasi-normal terms}] \dots - k\tau_{jkl} \quad (76)$$

where  $k$  is a positive constant. The damping coefficient,  $k$ , could be a function of time, energy density, other statistical quantities, or any number of things but for our purpose an absolute constant is preferred. One is not completely in the dark as to the numerical value of  $k$  since it has dimensions of  $(\text{time})^{-1}$ , and one would expect that the time scale of the dynamic features should be reflected in its value.

Results of calculations using eq (76) are shown in figures 22 and 23. The initial conditions were exactly those used in discussing the quasi-normal approximation, the Monte Carlo method, and the simple stochastic dynamic closure method earlier in this section. In figure 22, the damping coefficient is 0.1. Clearly, the eddy-damped theory is more congruent than the simpler closure scheme. Different values of the damping coefficient are used and the results compared in figure 23. The calculations are in very close

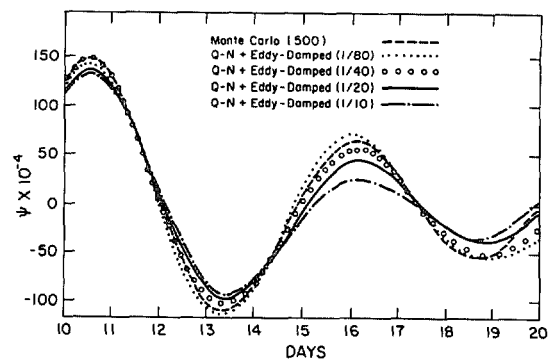


FIGURE 23.—Comparison of various eddy-damped closures by showing cosine components of wave 4.

agreement with the Monte Carlo results out to 18 days.

The extremely good results obtained with this simple damping factor certainly indicate that the technique is applicable to stochastic dynamic predictions. The additional calculations required for this method may not give sufficient improvement in the early stages of a forecast to warrant its use. However, recent turbulence calculations by Leith (1971) indicate that the effect of third moments being damped can be incorporated without calculating third moments at every time step. This approach, called "the eddy-damped Markovian approximation" is also discussed by Orszag (1971). The saving of computer time resulting from this method may make the eddy-damped quasi-normal closure approach to the stochastic dynamic equations economically feasible.

#### CLOSURE IN A DISPERSIVE SYSTEM

In his study of predictability, Lorenz (1965) assumed  $f$ , the Coriolis parameter, to be constant. Actually, on a global scale,  $f$  is a function of  $y$  and this dependence can be expressed as  $\beta = df/dy$ . Frequently,  $\beta$  is considered a constant with a numerical value appropriate for  $45^\circ$  latitude. The inclusion of the  $\beta$ -effect causes a significant change in the direction and amplitude of the phase speed of the ultra-long waves; however, the calculations presented in part II indicate that Lorenz' assumption was correct; that is, the  $\beta$ -effect is not important to predictability.

The  $\beta$ -effect gives rise to vortex forces or restoring forces which act to restore displaced fluid columns and move waves westward. The waves (Rossby waves) are dispersive; that is, the phase speeds are a function of the wavelength. A simple perturbation analysis yields the phase speed of these waves as  $\bar{u} - \beta/n^2$  where  $\bar{u}$  is the constant mean flow and  $n$  is the wave number. This shows that Rossby waves always travel westward relative to the mean flow and are highly dispersive, but for the higher wave numbers the  $\beta$ -term is less effective.

An interesting paper by Benney and Newell (1969) discusses the closure problem that results when trying to solve the statistical initial value problem for a system of waves. The system is assumed to be spatially homogeneous and the problem is to close the hierarchy of equations for the statistical moments. These authors claim that in a

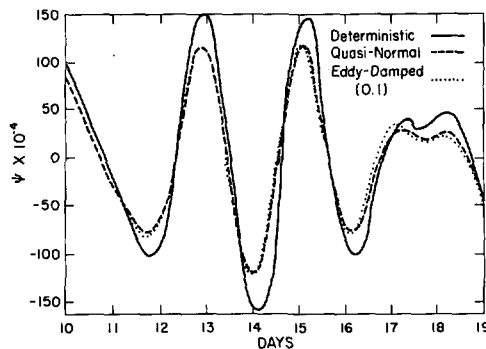


FIGURE 24.—Comparison of closure schemes with  $\beta$ -effect and waves 2, 4, and 6 by showing cosine components of wave 4.

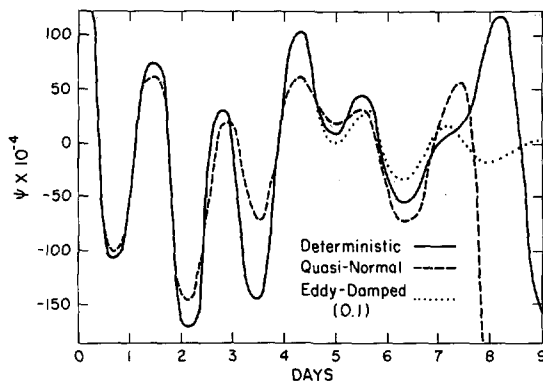


FIGURE 25.—Comparison of closure schemes with  $\beta$ -effect and waves 4, 8, and 12 by showing cosine components of wave 8.

weakly nonlinear system of dispersive waves there is a “natural” closure. The dispersive nature of the waves causes a decoupling of triple correlations and there is an approach to the Gaussian state, that is, a multivariate normal probability distribution. Benney and Newell postulate that a second process is at work regenerating higher moments by nonlinear couplings (due to the nonlinear inertial forces transferring energy between wave numbers), but that this second process occurs over longer time scales. It is of interest to test these ideas on a stochastic dynamic system with dispersive waves, but where homogeneity is not assumed.

The  $\beta$ -effect, introduced with the same initial conditions that were used in the quasi-normal calculation (cf. fig. 19), are used to give the results shown in figure 24. No negative energy occurs and figure 24 clearly shows that the quasi-normal closure method does not blow up. Moreover, the same calculation using the eddy-damped method with coefficient  $k=0.1$  agrees with the quasi-normal calculation almost exactly out to 16 days. Thus, the damping term is damping “nothing” or at least a very small quantity. A comparison of figures 19 and 24 reveals that the  $\beta$ -effect has introduced a fast time scale into the system, as expected with no artificial divergence.

The above results are for waves 2, 4, and 6 which are highly dependent upon  $\beta$ . Higher wave numbers are not so dependent. Figure 25 shows calculations with the same initial values as before but for the waves 4, 8, and 12.

The amplitude of the cosine term of wave 8 is shown. Here, one sees that the quasi-normal theory blows up after 8 days—the  $\beta$ -effect is not strong enough in these waves to give a natural closure. Note also that the results from the quasi-normal closure and the eddy-damped closure differ significantly from the deterministic solution after 6 days—both in amplitude and phase.

These calculations show that the discussion of Benney and Newell applies equally well to the stochastic dynamic prediction of the ultra-long waves. However, the practical application of numerical weather prediction must include much smaller scales or higher wave numbers than those where the  $\beta$ -effect is pronounced, so that the discussion of Benney and Newell is irrelevant for our purposes.

## 8. CONCLUSIONS

This paper has merely been an introduction into a few of the important concepts associated with the stochastic dynamic method. The formally exact stochastic approach to a nonlinear problem (with associated uncertainties) leads to an infinite unclosed set of moment equations. Epstein (1969b) has closed this system of equations in a very simple way. Calculations given here suggest that this closure may be sufficient for some applications. However, evidence has been presented that a better closure scheme should be used in extended time integrations.

The stochastic dynamic equations which neglect third and higher order moments conserve the ensemble energy in those cases where the energy should be deterministically conserved. However, the neglect of third moments was shown to lead to a misappropriation of energy between the uncertain energy components. The quasi-normal closure scheme fails to give realizable results in the stochastic dynamic equations just as it fails in homogeneous isotropic turbulence theory. The eddy-damped closure method gave extremely good results out to 18 days as compared with Monte Carlo calculations.

The stochastic dynamic approach treats the question of predictability or growth of uncertainty in an explicit manner. The use of the equations in considering the predictability of various scales of features is given in part II. We emphasize here that more can be provided than the usual notion of an average value of predictability. More important, the believability of the atmospheric variables (which depends upon all the dynamic processes at work and all the associated uncertainties) can be localized in space and time. In addition, the nature and amount of this growth can be viewed through the energetics of the stochastic dynamic equation set. Thus, a full energy description of the growth of error has been presented, if only in simple models.

There are two important implications concerning the stochastic approach that have been brought into focus in this study: (1) the method has value, and (2) the method is possible. We amplify on these in reverse order.

The stochastic equations can be solved. The computer power needed is monumental but not infinite. The infinite set of moments required in principle is not necessary in practice. It appears that the dynamical equations them-

selves damp the higher order moments. This was seen in the extremely accurate results obtained by a simple damping of third moments. This is obviously related to the fact that the original nonlinear equations were quadratic. The author has derived the stochastic equations for a general cubic deterministic equation set and the closure problem is more complex. The instability and energy transfer mechanisms in the quadratic hydrodynamic set involve triple correlations of deterministic variables. One might speculate that the absence of any known significant interaction of four or more variables accounts for the success of the closure used here.

The value of the stochastic approach lies not in its forecast of the mean of the dependent variables. In fact, in the early stages of the forecast, there will not be too much difference between these and the deterministically computed values of these variables. The value of the method shown here is its ability to forecast the uncertainty of the variables. We have shown that the stochastic equation set including third moments is energetically consistent. This means that the error growth is realistic and that the believability of each variable will evolve according to the dynamical situation at hand.

#### ACKNOWLEDGMENTS

The author is grateful to Professor Edward S. Epstein and Dr. C. E. Leith for their helpful suggestions.

Financial support was provided by the United States Air Force and by National Science Foundation grants GP-4385 and GS-19248. Computations were performed at the National Center for Atmospheric Research. The author thanks Mrs. Mary Daigle of the National Meteorological Center, National Weather Service, NOAA, for typing the manuscript.

#### REFERENCES

- Benny, D. J., and Newell, Alan C., "Random Wave Closures," *Studies in Applied Mathematics*, Vol. 48, No. 1, Massachusetts Institute of Technology Press, Cambridge, Mar. 1969, pp. 29-53.
- Dutton, John A., and Johnson, Donald R., "The Theory of Available Potential Energy and a Variational Approach to Atmospheric Energetics," *Advances in Geophysics*, Vol. 12, Academic Press, New York, N.Y., 1967, pp. 333-436.
- Edwards, S. F., "The Statistical Dynamics of Homogeneous Turbulence," *Journal of Fluid Mechanics*, Vol. 18, No. 2, Cambridge University Press, London, England, Feb. 1964, pp. 239-273.
- Epstein, Edward S., "The Role of Initial Uncertainties in Prediction," *Journal of Applied Meteorology*, Vol. 8, No. 2, Apr. 1969a, pp. 190-198.
- Epstein, Edward S., "Stochastic Dynamic Prediction," *Tellus*, Vol. 21, No. 6, Stockholm, Sweden, 1969b, pp. 739-757.
- Fleming, Rex J., "Concepts and Implications of Stochastic Dynamic Prediction," *NCAR Cooperative Thesis No. 22*, University of Michigan, Ann Arbor, and Laboratory of Atmospheric Science, National Center for Atmospheric Research, Boulder, Colo., 1970, 171 pp.
- Frieberger, Walter, and Grenander, Ulf, "On the Formulation of Statistical Meteorology," *Review of the International Statistical Institute*, Vol. 33, No. 1, Institute of Mathematical Statistics, University of Stockholm, Sweden, 1965, pp. 59-86.
- Gleeson, Thomas A., "A Causal Relation for Probabilities in Synoptic Meteorology," *Journal of Applied Meteorology*, Vol. 5, No. 3, June 1966, pp. 365-368.
- Hide, Raymond, "Some Experiments on Thermal Convection in a Rotating Liquid," *Quarterly Journal of the Royal Meteorological Society*, Vol. 79, No. 339, London, England, Jan. 1953, p. 161.
- Hildebrand, Francis B., *Advanced Calculus for Applications*, Prentice-Hall, Inc., Englewood Cliffs, N.J., 1965, 646 pp.
- Leith, C. E., "Numerical Simulation of Turbulent Flow," *Properties of Matter Under Unusual Conditions*, John Wiley & Sons, Inc., New York, N.Y., 1969, pp. 267-271.
- Leith, C. E., "Atmospheric Predictability and Two-Dimensional Turbulence," *Journal of the Atmospheric Sciences*, Vol. 28, No. 2, Mar. 1971, pp. 145-161.
- Lorenz, Edward N., "Energy and Numerical Weather Prediction," *Tellus*, Vol. 12, No. 4, Stockholm, Sweden, Nov. 1960, pp. 364-373.
- Lorenz, Edward N., "Deterministic Nonperiodic Flow," *Journal of the Atmospheric Sciences*, Vol. 20, No. 2, Mar. 1963a, pp. 130-141.
- Lorenz, Edward N., "The Mechanics of Vacillation," *Journal of the Atmospheric Sciences*, Vol. 20, No. 5, Sept. 1963b, pp. 448-464.
- Lorenz, Edward N., "A Study of the Predictability of a 28-Variable Atmospheric Model," *Tellus*, Vol. 17, No. 3, Aug. 1965, pp. 321-333.
- Lorenz, Edward N., "The Predictability of a Flow Which Possesses Many Scales of Motion," *Tellus*, Vol. 21, No. 3, 1969, pp. 289-307.
- Millionshtebikov, M., "On the Theory of Homogeneous Isotropic Turbulence," *Compte Rendus (Doklady) de l'Academie Des Sciences de l'U.R.S.S.*, Vol. 32, Moscow, U.S.S.R., 1941, pp. 615-618.
- Ogura, Yoshimitsu, "A Consequence of the Zero-Fourth-Cumulant Approximation in the Decay of Isotropic Turbulence," *Journal of Fluid Mechanics*, Vol. 16, No. 1, Cambridge University Press, London, England, May 1963, pp. 33-40.
- Orszag, Steven A., "Analytical Theories of Turbulence," *Journal of Fluid Mechanics*, Vol. 41, No. 2, Cambridge University Press, London, England, Apr. 1970, pp. 363-386.
- Proudman, Ian, and Reid, W. H., "On the Decay of a Normally Distributed and Homogeneous Turbulent Velocity Field," *Philosophical Transactions of the Royal Society of London*, Ser. A, Vol. 247, No. 926, England, Nov. 4, 1954, pp. 163-189.
- Tatarskii, V. I., "The Use of the Dynamical Equations in the Probability Forecast of the Pressure Field," *Atmospheric and Oceanic Physics*, Vol. 5, No. 3, The American Geophysical Union, Washington, D.C. Mar. 1969, pp. 162-164 (translation of "Ispol'zovanie Dinamicheskikh Uravnenii Pri Veroiatnostnom Prognoze Baricheskogo Polia," *Akademiia Nauk SSSR, Izvestiia, Fizika Atmosfery i Okeana*, Vol. 5, No. 3, Leningrad, U.S.S.R. Mar. 1969, pp. 293-297).
- Taylor, Geoffrey Ingram, "Diffusion by Continuous Movement," *Proceedings of the London Mathematical Society*, Vol. 20, London Mathematical Society, London, England, 1921, pp. 196-212.
- Thompson, Philip Duncan, "Uncertainty of Initial State as a Factor in the Predictability of Large-Scale Atmospheric Flow Patterns," *Tellus*, Vol. 9, No. 3, Stockholm, Sweden, Aug. 1957, pp. 275-295.
- Wiin-Nielsen, Aksel, "On Short- and Long-Term Variations in Quasi-Barotropic Flow," *Monthly Weather Review*, Vol. 89, No. 11, Nov. 1961, pp. 461-476.
- Wiin-Nielsen, Aksel, "Some New Observational Studies of Energy and Energy Transformations in the Atmosphere," *World Meteorological Organization Technical Note No. 66*, Geneva, Switzerland, 1965, pp. 177-202.
- Wiin-Nielsen, Aksel, "On the Annual Variation and Spectral Distribution of Atmospheric Energy," *Tellus*, Vol. 19, No. 4, Stockholm, Sweden, Nov. 1967, pp. 540-559.
- Wiin-Nielsen, Aksel, "On the Intensity of the General Circulation of the Atmosphere," *Reviews of Geophysics*, Vol. 6, No. 4, Nov. 1968, pp. 559-579.